
Mobilizing Personalized Federated Learning in Infrastructure-Less and Heterogeneous Environments via Random Walk Stochastic ADMM

Ziba Parsons
CIS Department
University of Michigan
Dearborn, MI
zibapars@umich.edu

Fei Dou
School of Computing
University of Georgia
Athens, GA
fei.dou@uga.edu

Houyi Du
CIS Department
University of Michigan
Dearborn, MI
houyidu@umich.edu

Zheng Song
CIS Department
University of Michigan
Dearborn, MI
zhesong@umich.edu

Jin Lu
School of Computing
University of Georgia
Athens, GA
jin.lu@uga.edu

Abstract

This paper explores the challenges of implementing Federated Learning (FL) in practical scenarios featuring isolated nodes with data heterogeneity, which can only be connected to the server through wireless links in an infrastructure-less environment. To overcome these challenges, we propose a novel mobilizing personalized FL approach, which aims to facilitate mobility and resilience. Specifically, we develop a novel optimization algorithm called Random Walk Stochastic Alternating Direction Method of Multipliers (RWSADMM). RWSADMM capitalizes on the server's random movement toward clients and formulates local proximity among their adjacent clients based on hard inequality constraints rather than requiring consensus updates or introducing bias via regularization methods. To mitigate the computational burden on the clients, an efficient stochastic solver of the approximated optimization problem is designed in RWSADMM, which provably converges to the stationary point almost surely in expectation. Our theoretical and empirical results demonstrate the provable fast convergence and substantial accuracy improvements achieved by RWSADMM compared to baseline methods, along with its benefits of reduced communication costs and enhanced scalability.

1 Introduction

Federated Learning (FL) [43, 29, 30, 31] is a distributed machine learning paradigm that enables clients to learn a shared model without sharing their private data. Unlike traditional machine learning approaches that rely on central servers for model training, FL allows clients to collaborate and train the model in a distributed manner, overcoming privacy issues related to passing data to a central server. Despite its advancements, real-world applications in environments with insufficient network support continue to face challenges. a) Maintaining consistent and reliable connections between the central server and clients becomes exceedingly challenging in environments lacking network infrastructures, e.g., natural disasters or military warzones. While intermittent connectivity may be available through satellite networks, the instability and limited capacity of such networks prevent the transmission of large data volumes, making it difficult to collect model updates from soldiers or first responders. b) The non-IID (non-independent and identically distributed) nature of clients' data, characterized by heterogeneity across the network, can hinder the generalization of the global model for each client. Addressing these challenges is crucial for practical FL in such environments. In this paper, we propose RWSADMM, a novel FL scheme that uses Random Walk (RW) algorithm to

enable server mobility among client clients. These dynamic approach benefits scenarios with limited internet connectivity, where clients form clusters using local short-range transmission devices.

For instance, in the context of a warzone, we consider a scenario where soldiers are equipped with integrated visual augmentation systems (IVAS) [5]. To facilitate the collection of model updates from the soldiers, a tactical vehicle equipped with a powerful computer navigates the warzone [4], communicating with soldiers' locations through a satellite network. Upon reaching a soldier, the tactical vehicle employs short-range communication technologies such as WiFi direct, Zigbee [6], or Bluetooth to establish connections with nearby IVAS devices. Through these connections, the tactical vehicle collects model updates from the soldiers and distributes new models as necessary. A graph-based representation is employed to determine the order of interactions with soldiers, where soldiers are depicted as nodes, and the edge between a soldier and its neighbor indicates that the neighbor is within the communication range of the vehicle that reaches the soldier. This graph assists the tactical vehicle in making informed decisions about the order in which it engages with the soldiers.

Other applicable examples of such constrained network situations include ad hoc wireless learning [61, 62, 63], wildlife tracking [54, 55, 56], Internet of Underwater Things (IoUT) [58, 57], natural disaster management [59, 60], warzones [66], or creating a digital democracy [65, 68] which assists in overcoming restrictions imposed by totalitarian regimes that prohibit internet access to civilians.

Specifically, to address challenge a), we propose an algorithmic framework called RWSADMM (Fig. 1), short for Random Walk Alternating Directional method of Multipliers, which considers a dynamic reachability graph among distributed clients using a movable vehicle as the central server. Clients are represented as nodes in the graph, with edges denoting neighborhood connections. Personal devices, referred to as local clients, establish dynamic connectivity with the server when the server is nearby. The server connects with a selected client and its neighbors while moving between locations using a non-homogeneous RW algorithm for probabilistic navigation. In each computation round, the vehicle broadcasts and gathers local model updates from residing clients, who rely on short-range communication to interact with the moving server, when it's within the communication range. The received updates are aggregated and used to update the global model iteratively.

To tackle the second challenge (b) arising from the heterogeneity of data distribution among clients, RWSADMM incorporates model personalization through local proximity among adjacent clients using hard inequality constraints, as opposed to unconstrained optimization with regularization techniques that may induce model bias. By formulating the problem with these constraints, RWSADMM reduces the computational complexity for clients, effectively mitigating the limitations of local computational power. This is achieved by designing the solver to the stochastic approximation of the minimization subproblem within the typical ADMM algorithm.

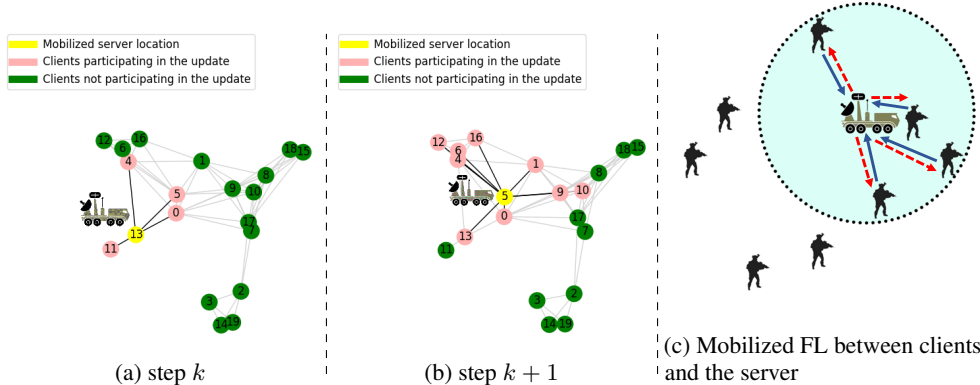


Figure 1: This illustration showcases the training process using the RWSADMM algorithm. A vehicle, serving as the mobile server, navigates between different clients using a random walk strategy. (a) In step k , the server moves to client 13, covering the clients in $\mathcal{N}(13)$ for FL model training and completing the aggregation step. (b) In step $k + 1$, client 5 is selected, and the vehicle moves to client 5. The training and aggregation steps occur within the zone encompassing $\mathcal{N}(5)$.

Our research makes three main contributions. Firstly, our proposed RWSADMM algorithm is **the first attempt to enable mobilizing FL with efficient communication and computation in an infrastructure-less setting**. The RWSADMM framework involves a server dynamically moving between different regions of clients and receiving updates from one or a few clients residing in the

selected zone, which reduces communication costs and enhances system flexibility. Secondly, to address the issue of data heterogeneity among clients, RWSADMM **formulates local proximity among adjacent clients based on hard inequality constraints, avoiding the introduction of model bias via consensus updates**. This approach provides an alternative realization of personalization, which is crucial when dealing with highly heterogeneous data distributions. Thirdly, to mitigate the computational burden on the clients, an efficient stochastic solver of the subproblem is designed in RWSADMM, which **provably converges to the stationary point almost surely in expectation** under mild conditions independent of the data distributions. Our theoretical and empirical results demonstrate the superiority of our proposed algorithm over state-of-the-art personalized Federated Learning (FL) algorithms, providing empirical evidence for the effectiveness of our approach.

2 Related Work

This paper is relevant to two distinct research areas, which are reviewed in two separate sections: FL frameworks that tackle data heterogeneity and ADMM-based FL frameworks.

FL with data heterogeneity FL was initially introduced as FedAvg, a client-server-based framework that didn't allow clients to personalize the global model to their local data [43]. This led to poor convergence due to local data heterogeneity, negatively impacting the global FL model's performance on individual clients. Recent works proposed a two-stage approach to personalize the global model. In the first stage, the FL global model is trained similarly to FedAvg. However, the second stage is included to personalize the global model for each local client through additional training on their local data. [21] demonstrated that FedAvg is equivalent to Reptile, a new meta-learning algorithm, when each client collects the same amount of local data. To learn a global model that performs well for most participating clients, [20] proposed an improved version, Per-FedAvg. This new variant aims to learn a good initial global model that can adapt quickly to local heterogeneous data. An extension of Per-FedAvg, called pFedMe [19], introduced an ℓ_2 -norm regularization term to balance the agreement between local and global models and the empirical loss. [52] proposed Ditto, a multi-task learning-based FL framework that provides personalization while promoting fairness and robustness to byzantine attacks. Ditto uses a regularization term to encourage personalized local models to be close to the optimal global model. [64] proposed to interpolate local and global models to train local models while also contributing to the global model. However, scaling these approaches can be challenging due to high communication costs, reliance on strong assumptions about network connectivity, or the requirement to compute second-order gradients. Additionally, there is a potential for enhancing the algorithms' overall performance.

ADMM-based FL The Alternating Direction Method of Multipliers (ADMM) is a widely recognized algorithm that effectively tackles optimization problems across multiple domains. In recent studies, ADMM has been successfully employed in distributed learning, as demonstrated by several works [11, 12, 13, 14, 15, 16, 17, 18]. In Federated Learning (FL) context, researchers have proposed various methods to address specific challenges. For handling falsified data in Byzantine settings, [10] introduced a robust ADMM-based approach. To mitigate local computational burdens in FL, [9] developed an inexact ADMM-based algorithm suitable for edge learning configurations. FL itself enables local training without the need to share personal data between clients and the server. Despite the advantages of FL, there is still a concern regarding clients' privacy. Analyzing the parameter differences in the trained models uploaded by each client can compromise their privacy. To tackle this issue, [8] proposed an inexact ADMM-based federated learning algorithm that incorporates differential privacy (DP) techniques [7]. By leveraging DP, the algorithm enhances privacy protection during the FL process. These ADMM-based frameworks also have high communication costs, ranging from $O(n)$ to $O(n^2)$ per iteration, depending on the network's density with n clients. [67] introduced a Proximal Primal-Dual Algorithm (Prox-PDA) to enable network nodes to compute the set of first-order stationary solutions collectively. Moreover, these algorithms do not account for data heterogeneity in their framework designs, leading to performance deterioration in such scenarios. The most similar algorithm to RWSADMM is called Walkman [35]. Walkman is an ADMM-based framework utilizing the random walk technique for distributed optimization. In Walkman, the communication and computation costs are reduced by activating only one agent at each step. Compared to other ADMM-based approaches, including Walkman, RWSADMM has several distinctive features. RWSADMM leverages stochastic approximation to reduce computation costs per iteration and enforces hard inequality constraints instead of consensus to manage heterogeneous data, resulting in increased robustness. Additionally, RWSADMM considers the dynamic graph,

allowing it to adapt to changing network conditions and potentially improve communication efficiency. RWSADMM also incorporates a hard constraint parameter ϵ to promote local proximity among clients instead of using a regularization term as Walkman does to promote client consensus. This approach better balances personalization and global optimization. Finally, while Walkman is fully distributed without server involvement, RWSADMM is a server-based approach in which the server aggregates information from a small group of clients in each computation round.

3 Random Walk Stochastic ADMM (RWSADMM)

Before delving into the specifics of the proposed algorithm, we present the key notation used throughout this research. $\mathbf{x} \in \mathbb{R}^d$ represents a vector with length d and \mathbf{e} is defined as a vector with entries equal to 1 and $\mathbf{X} \in \mathbb{R}^{l \times d}$ depicts a matrix with l rows and d columns. $[\mathbf{x}]_i$ represents the i th element of vector \mathbf{x} and $[\mathbf{X}]_{ij}$ is the (i, j) th element of matrix \mathbf{X} . $[\mathbf{X}]_i, [\mathbf{X}]^j$ represent the i th row and j th column of matrix \mathbf{X} , respectively. $(\nabla f(\mathbf{x}))_j$ is used to denote the j th entry of the gradient of $f(\mathbf{x})$. The inner product of A and B is shown as $\langle A, B \rangle$. $\mathbb{E}_t[\cdot]$ indicates the expectation given the past ξ_1, \dots, ξ_{t-1} . \odot represents the Hadamard product/element-wise product and \otimes represents the Kronecker product between two matrices. Finally, Norm p of vector \mathbf{x} is denoted as $\|\mathbf{x}\|_p^p = \sum_{i=1}^d |x_i|^p$, $\mathbf{x} \in \mathbb{R}^d$ and Frobenius norm of matrix \mathbf{X} is written as $\|\mathbf{X}\|_F = \sqrt{\sum_{i=1}^n \sum_{j=1}^m |x_{ij}|^2}$.

Let us first define our Mobilizing FL problem. Mobilizing FL, which involves a mobile server, can be formulated as an optimization problem on a connected graph $\mathcal{G} = (\mathcal{V}, \mathcal{E})$. The graph comprises a set of n clients, represented as $\mathcal{V} = v_1, v_2, \dots, v_n$, and a set of m edges, denoted as \mathcal{E} . The objective is to minimize the average loss function across all clients while adhering to inequality constraints that ensure local proximity among the clients' respective local models. The optimization problem can be formulated mathematically as follows:

$$\min_{\mathbf{x}_{1:n} \in \mathbb{R}^p} \frac{1}{n} \sum_{i=1}^n f_i(\mathbf{x}_i) \quad s.t. \quad |\mathbf{x}_i - \mathbf{x}_j| \leq \epsilon_i, \forall i \in \{1, \dots, n\}, \forall j \in \mathcal{N}(i)/v_i. \quad (1)$$

where $f_i(\mathbf{x}_i)$ represents the local loss function with the model parameter as \mathbf{x}_i for the client i , the vertex set $\mathcal{N}(i)$ contains client i and its neighboring clients, and ϵ_i is the non-consensus relaxation between local neighboring clients to replace model consensus requirement in typical FL. In our proposed FL method, we model the server's movement as a dynamic Markov Chain, introducing a dynamic element to the traditional ADMM-based approach. This work is the first to consider a dynamic mobile server within the ADMM-based FL framework. In RWSADMM, client-server communication occurs only when the server is close to a client. The sequence of client indices that are updated, denoted as i_k , evolves based on a non-homogeneous Markov Chain with a state space of $1, \dots, n$ [32]. To describe the transition dynamics of the Markov Chain, we employ the non-homogeneous Markovian transition matrix $\mathbf{P}(k)$, which represents the probabilities of transitioning between clients at time k . Specifically, the conditional probability of selecting client j as the next client, given that client i is the current client, is defined as:

$$[\mathbf{P}(k)]_{i,j} = Pr \{i_{k+1} = j | i_k = i\} \in [0, 1] \quad (2)$$

Additionally, it is assumed that the server determines the probability of all possible locations for its next destination based on the transition matrix $\mathbf{P}(k)$ at time k . This provides a probabilistic approach to server navigation, allowing it to move around the network more effectively. To guarantee convergence, RWSADMM depends on the frequency of revisiting each agent. This quality is described by the *mixing time* of the algorithm. An assumption for the mixing time is as follows:

Assumption 3.1. The random walk $(i_k)_{k \geq 0}, v_{i_k} \in \mathcal{V}$ forms an irreducible and aperiodic (ergodic) Markov Chain with transition probability matrix of $\mathbf{P}(k) \in \mathbb{R}^{n \times n}$ defined in Eq. (2) and stationary distribution $\boldsymbol{\pi}$ satisfying $\lim_{k \rightarrow \infty} \boldsymbol{\pi}^T \mathbf{P}(k) = \boldsymbol{\pi}^T$. The mixing time (for a given $\delta > 0$) is defined as the smallest integer $\tau(\delta)$ such that $\forall i \in \mathcal{V}$,

$$\left\| [\mathbf{P}(k)^{\tau(\delta)}]_i - \boldsymbol{\pi}^T \right\| \leq \delta \pi_* \quad (3)$$

where $\pi_* := \min_{i \in \mathcal{V}} \pi_i$. This inequality states the fact that regardless of the current state i and time k , the probability of visiting each state j after $\tau(\delta)$ steps is $(\delta \pi_*)$ -close to π_j , that is, $\forall i, j \in \mathcal{V}$,

$$\left\| [\mathbf{P}(k)^{\tau(\delta)}]_{ij} - \pi_j \right\| \leq \delta \pi_* \quad (4)$$

Eq. (4) is used to prove the sufficient descent of a Lyapunov function L_β in Section 3.1. Let's also define

$$\mathbf{P}_{max} = \lim_{k \rightarrow +\infty} \{\mathbf{P}[\mathbf{P}]_{ij} = \max_k [\mathbf{P}(k)]_{ij}\}, \quad (5)$$

from which one can further obtain $\|\mathbf{P}(k)\| \leq \|\mathbf{P}_{max}\|$ for all k . Namely, the matrix \mathbf{P}_{max} is computed as the element-wise maximum matrix among all the matrices $\mathbf{P}(k)$, for $k = 0, \dots, \infty$. Therefore, the mixing time requirement in Eq. (3) is guaranteed to hold for

$$\tau(\delta) = \lceil \frac{1}{1 - \sigma(\mathbf{P})} \ln \frac{\sqrt{2}}{\delta \pi_*} \rceil \stackrel{(a)}{\leq} \lceil \frac{1}{1 - \sigma(\mathbf{P}_{max})} \ln \frac{\sqrt{2}}{\delta \pi_*} \rceil \quad (6)$$

where $\sigma(\mathbf{P}) := \sup\{\|f^T \mathbf{P}\| / \|f\| : f^T \mathbf{1} = 0, f \in \mathbb{R}^n\}$. Using Eq. (5), we have $\forall \mathbf{P}$, $\sigma(\mathbf{P}) \leq \sigma(\mathbf{P})_{max}$ and the inequality (a) can be inferred.

3.1 Algorithm

In this section, we derive RWSADMM by integrating random walk and stochastic inexact approximation techniques into ADMM. Considering $\mathbf{X} := row(\mathbf{x}_1, \mathbf{x}_2, \dots, \mathbf{x}_n) \in \mathbb{R}^{p \times n}$, $F(\mathbf{X}) := \sum_{i=1}^n f_i(\mathbf{x}_i)$, where the operation $row(\cdot)$ refers to row-wise stacking of vectors \mathbf{x}_i 's. The mobilizing FL problem (1) can be expressed as:

$$\min_{\mathbf{y}_{1:n}, \mathbf{X}} \frac{1}{n} F(\mathbf{X}) \quad \text{s.t.} \quad |\mathbf{1} \otimes \mathbf{y}_i - \mathbf{X}_{\mathcal{N}(i)}| \leq \mathbf{1} \otimes \epsilon_i / 2, \forall i = 1, \dots, n \quad (7)$$

where $\mathbf{1} = [1 \ 1 \ \dots \ 1] \in \mathbb{R}^{n_i}$, n_i denotes the volume of the vertex set $\mathcal{N}(i)$. The constraint implies that $|\mathbf{x}_i - \mathbf{x}_j| \leq \epsilon_i$, $\forall i = 1 \dots n$ and $\forall j \in \mathcal{N}(i)$ through the triangle inequality. \mathbf{y}_i stored on the server is necessarily introduced as a local proximity of $\mathcal{N}(i)$. We can obtain the augmented Lagrangian for problem (7)

$$L_\beta(\mathbf{y}_{1:n}, \mathbf{X}, \mathbf{Z}_{1:n}) = \frac{1}{n} [F(\mathbf{X}) + \sum_{i=1}^n \langle \mathbf{Z}_i, |\mathbf{1} \otimes \mathbf{y}_i - \mathbf{X}_{\mathcal{N}(i)}| - \epsilon_i \rangle + \frac{\beta}{2} \sum_{i=1}^n \||\mathbf{1} \otimes \mathbf{y}_i - \mathbf{X}_{\mathcal{N}(i)}| - \epsilon_i\|_F^2] \quad (8)$$

where $\epsilon_i = \epsilon_i / 2$ and $\mathbf{Z}_i \in \mathbb{R}^{n_i p}$ are the dual variable and $\beta > 0$ is the barrier parameter. The RWSADMM algorithm minimizes the augmented Lagrangian $L_\beta(\mathbf{y}_{1:n}, \mathbf{X}, \mathbf{Z}_{1:n})$ in an iterative manner. At each iteration k , only a subset of clients covered by the mobilized server, the clients in $\mathcal{N}(i_k)$, participate in the federated update. The following updates are performed:

$$\mathbf{x}_{i_k} = \arg \min_{\mathbf{x}_{i_k}} L_\beta(\mathbf{y}'_{i_k}, \mathbf{x}_{i_k}, \mathbf{z}'_{i_k}), \quad \mathbf{y}_{i_k} = \arg \min_{\mathbf{y}_{i_k}} L_\beta(\mathbf{y}_{i_k}, \mathbf{X}_{\mathcal{N}(i_k)}, \mathbf{Z}'_{\mathcal{N}(i_k)}),$$

where \mathbf{y}'_{i_k} , \mathbf{x}_{i_k} , and \mathbf{z}'_{i_k} denote the groups of variables of the local parameters stored by client i_k at the $(k-1)$ th update. After solving these subproblems, we update the multiplier \mathbf{z}_{i_k} as follows:

$$\mathbf{z}_{i_k} = \mathbf{z}'_{i_k} + \beta(|\mathbf{y}_{i_k} - \mathbf{x}_{i_k}| - \epsilon_i),$$

Next, we derive the solver of each subproblem. The three steps are noted as Updating \mathbf{x}_{i_k} , Updating \mathbf{y}_{i_k} , and Updating \mathbf{z}_{i_k} .

$$\text{Updating } \mathbf{x}_{i_k}: \quad \min_{\mathbf{x}_{i_k}} \left[f_{i_k}(\mathbf{x}_{i_k}) + \langle \mathbf{z}'_{i_k}, |\mathbf{y}'_{i_k} - \mathbf{x}_{i_k}| - \epsilon_{i_k} \rangle + \frac{\beta}{2} \||\mathbf{y}'_{i_k} - \mathbf{x}_{i_k}| - \epsilon_{i_k}\|_2^2 \right] \quad (9)$$

The Problem (9) can be solved iteratively, consuming significant computational resources for the local clients. Furthermore, the computational complexity increases as the local dataset grows, as is often true in real-world applications. By utilizing the stochasticity and first-order subgradient expansion, we arrive at a more computationally efficient approximation of the original problem in Eq. (10).

$$\min_{\mathbf{x}_{i_k}} \left[g_{i_k}(\mathbf{x}'_{i_k}, \boldsymbol{\xi}_{i_k})(\mathbf{x}_{i_k} - \mathbf{x}'_{i_k}) + \langle \mathbf{z}'_{i_k}, |\mathbf{y}'_{i_k} - \mathbf{x}_{i_k}| - \epsilon_{i_k} \rangle + \frac{\beta}{2} \||\mathbf{y}'_{i_k} - \mathbf{x}_{i_k}| - \epsilon_{i_k}\|_2^2 \right] \quad (10)$$

In Eq. (10), $\boldsymbol{\xi}_{i_k}$ denotes one or a few samples randomly selected by client i_k from its feature set and their ground truth labels in pairs at the k -th iteration. The function $g_{i_k}(\mathbf{x}'_{i_k}, \boldsymbol{\xi}_{i_k})$ is defined as the stochastic gradient of $f_{i_k}(\mathbf{x}'_{i_k})$ at \mathbf{x}'_{i_k} . The stochastic approximation can tremendously reduce memory consumption and save computational costs in each iteration. By setting the subgradient of the objective function in Eq. (10) to zero, we can derive the closed-form solution in Eq. (11).

$$\mathbf{x}_{i_k} = \mathbf{y}'_{i_k} + \frac{1}{\beta} \mathbf{z}'_{i_k} \odot \text{sgn}(\mathbf{t}') - \frac{1}{\beta} \text{sgn}(\mathbf{t}') \odot (\epsilon_i + g_{i_k}(\mathbf{x}'_{i_k}, \boldsymbol{\xi}_{i_k})) = \mathbf{y}'_{i_k} + \frac{1}{\beta} \text{sgn}(\mathbf{t}') \odot (\mathbf{z}'_{i_k} - \epsilon_i - g_{i_k}(\mathbf{x}'_{i_k}, \boldsymbol{\xi}_{i_k})) \quad (11)$$

where the signum function $\text{sgn}(\cdot)$ extracts the signs of a vector and $\mathbf{t}'_{i_k} = \mathbf{y}'_{i_k} - \mathbf{x}'_{i_k}$.

Updating \mathbf{y}_{i_k} : We solve the following problem

$$\min_{\mathbf{y}_{i_k}} \langle \mathbf{Z}_{\mathcal{N}(i_k)}, |\mathbf{1} \otimes \mathbf{y}_{i_k} - \mathbf{X}_{\mathcal{N}(i_k)}| - \mathbf{1} \otimes \boldsymbol{\varepsilon}_{i_k} \rangle + \frac{\beta}{2} \|\mathbf{1} \otimes \mathbf{y}_{i_k} - \mathbf{X}_{\mathcal{N}(i_k)}| - \mathbf{1} \otimes \boldsymbol{\varepsilon}_{i_k}\|_F^2 \quad (12)$$

one can readily derive a closed-form solution for the problem (12) as:

$$\mathbf{y}_{i_k} = \frac{1}{n_{i_k}} \sum_{j \in \mathcal{N}_{i_k}} [\mathbf{x}_{i_k} - (\frac{\mathbf{z}_{i_k}}{\beta} + \boldsymbol{\varepsilon}_{i_k}) \odot \text{sgn}(\mathbf{t}_{i_k})] \quad (13)$$

where $\mathbf{t}_{i_k} = \mathbf{y}'_{i_k} - \mathbf{x}_{i_k}$ is similar to that of Eq. (11) except the updated \mathbf{x} . Specifically, via mathematical induction, we can attain the new updated form of \mathbf{y}_{i_k} below, which can also reduce the communication cost from $O(n)$ to $O(1)$:

$$\mathbf{y}_{i_k} = \mathbf{y}'_{i_k} + \frac{1}{n_{i_k}} [\mathbf{x}_{i_k} - (\frac{\mathbf{z}_{i_k}}{\beta} + \boldsymbol{\varepsilon}_{i_k}) \odot \text{sgn}(\mathbf{t}_{i_k})] - [\mathbf{x}'_{i_k} - (\frac{\mathbf{z}'_{i_k}}{\beta} + \boldsymbol{\varepsilon}_{i_k}) \odot \text{sgn}(\mathbf{t}'_{i_k})] \quad (14)$$

Updating \mathbf{z}_{i_k} : The Lagrangian multiplier \mathbf{z}_{i_k} can be updated strictly following the standard ADMM scheme below:

$$\mathbf{z}_{i_k} = \mathbf{z}'_{i_k} + \kappa\beta [\mathbf{x}_{i_k} - \mathbf{y}'_{i_k} - \boldsymbol{\varepsilon}_{i_k}] \quad (15)$$

The κ coefficient used in Eq. (15) is decayed in each process step to achieve better convergence.

Please refer to Appendix A for the entire RWSADMM algorithm framework.

4 Theoretical Analysis

In this section, we present the theoretical convergence guarantee of RWSADMM. To ensure its convergence, certain common assumptions are made regarding the properties of the loss functions. The assumptions are as follows:

Assumption 4.1. The objective function $f(\mathbf{x})$ is bounded from below and coercive over \mathbb{R}^p , that is, for any sequence $\{\mathbf{x}^k\}_{k \geq 0} \subset \mathbb{R}^p$,

$$\text{if } \|\mathbf{x}^k\| \xrightarrow{k \rightarrow \infty} \infty \Rightarrow \frac{1}{n} \sum_{i=1}^n f_i(\mathbf{x}) \rightarrow \infty \quad (16)$$

Assumption 4.2. The objective function $f_i(\mathbf{x})$'s are L-smooth, that is, f_i are differentiable, and its gradients are L-Lipschitz, that is, $\forall \mathbf{u}, \mathbf{v} \in \mathbb{R}^p$ [35],

$$\|\nabla f_i(\mathbf{u}) - \nabla f_i(\mathbf{v})\| \leq L\|\mathbf{u} - \mathbf{v}\|, \quad \forall i = 1, \dots, n \quad (17)$$

Remark: In consequence it also holds that $\forall \mathbf{u}, \mathbf{v} \in \mathbb{R}^p$

$$f_i(\mathbf{u}) - f_i(\mathbf{v}) \leq \nabla f_i(\mathbf{v})^T (\mathbf{u} - \mathbf{v}) + \frac{L}{2} \|\mathbf{u} - \mathbf{v}\|^2, \quad \forall i = 1, \dots, n. \quad (18)$$

Assumption 4.3. The objective function f is M-Lipschitz, that is, $\forall \mathbf{u}, \mathbf{v} \in \mathbb{R}^p$ [37],

$$|f(\mathbf{u}) - f(\mathbf{v})| \leq M\|\mathbf{u} - \mathbf{v}\| \quad (19)$$

Assumption 4.4. The first-order stochastic gradient is sampled, which returns a noisy but unbiased estimate of the gradient of f at any point $\mathbf{x} \in \mathbb{R}^p$, that is, $\forall \mathbf{x} \in \mathbb{R}^p$,

$$\mathbb{E}_{\xi}[g(\mathbf{x}, \xi)] = \nabla f(\mathbf{x}) \quad (20)$$

Remark: Substituting Eq. (20) into Eq. (17), one can obtain that for $i = 1, \dots, n$, we have

$$\|\mathbb{E}_{\xi}[g(\mathbf{u}, \xi)] - \mathbb{E}_{\xi}[g(\mathbf{v}, \xi)]\| \leq L\|\mathbf{u} - \mathbf{v}\| \quad (21)$$

Substituting Eq. (20) into Eq. (18), for $i = 1, \dots, n$, we can obtain

$$f_i(\mathbf{u}) - f_i(\mathbf{v}) \leq \mathbb{E}_{\xi}[g(\mathbf{v}, \xi)]^T (\mathbf{u} - \mathbf{v}) + \frac{L}{2} \|\mathbf{u} - \mathbf{v}\|^2, \quad (22)$$

Assumption 4.5. The noise variance of the stochastic gradient is bounded as:

$$\mathbb{E}_\xi(\|\nabla f(\mathbf{x}) - g(\mathbf{x}, \xi)\|^2) \leq \exp(1), \text{ for all } \mathbf{x}. \quad (23)$$

This condition bounds the expectation of $\|\nabla f(\mathbf{x}_t) - g(\mathbf{x}_t, \xi_t)\|^2$. Using Jensen's inequality, this condition implies a bounded variance [37].

We revisit the related crucial properties of the Markov Chain. The first time that the Markov Chain $(i_k)_{k \geq 0}$ hits agent i is denoted as $T_i := \min\{k : i_k = i\}$, and maximum value of T over all clients is defined as $T := \max\{T_1, \dots, T_n\}$. For $k > T$, let $\tau(k, i)$ denote the iteration of the last visit to agent i before k , mathematically we have

$$\tau(k, i) = \max\{k' : i_{k'} = i, k' < k\}. \quad (24)$$

To prove the convergence of our proposed algorithm, two Lyapunov functions defined for RWSADMM are required to be investigated:

$$L_\beta^k := L_\beta(\mathbf{y}^k, \mathbf{X}^k; \mathbf{Z}^k), \quad M_\beta^k := L_\beta^k + \frac{L^2}{n} \sum_{i=1}^n \left\| \mathbf{y}_i^{\tau(k,i)+1} - \mathbf{y}_i^{\tau(k,i)} \right\|^2 \quad (25)$$

where $L_\beta(\mathbf{y}^k, \mathbf{X}^k; \mathbf{Z}^k)$ is defined in Eq. (8). The M_β^k is utilized in the convergence analysis. To guarantee the convergence of our algorithm, first, we refer to the asymptotic analysis of the nonhomogeneous Markov chain presented in [46]. Define $\Phi(k, l)$ with $k \geq l$ as the product of the transition probability matrices for the Markov chain from time l to k , i.e., $\Phi(k, l) = \mathbf{P}(k) \dots \mathbf{P}(l)$ with $k \geq l$. Then we have the following convergence result:

Lemma 4.6. Consider

1. $\forall s, \lim_{k \rightarrow \infty} \Phi(k, l) = \frac{1}{n} \mathbf{e} \mathbf{e}^T$.
2. The convergence of Φ is geometric and the rate of convergence considering $\forall k, l$, with $k \geq l \geq 0$, is given by

$$|[\Phi(k, l)]_{i,j} - \frac{1}{n}| \leq \left(1 - \frac{\eta}{4n^2}\right)^{\lceil \frac{k-l+1}{Q} \rceil - 2} \quad (26)$$

Using Lemma 4.6, the convergence analysis of the algorithm is as follows.

Lemma 4.7. Under Assumptions 4.1 and 4.2, if $\beta > 2L^2 + L + 2$, $(M_\beta^k)_{k \geq 0}$ is lower bounded and convergent, the iterates $(\mathbf{y}^k, \mathbf{X}^k, \mathbf{Z}^k)_{k \geq 0}$ generated by RWSADMM is bounded.

The proof sketch and the detailed convergence proof are presented in Appendix B. Using Lemma 4.7 and B.6, we can present the convergence of RWSADMM in Theorem 4.8.

Theorem 4.8. Let Assumption 4.5 hold. For $\beta > 2L^2 + L + 2$, it holds that any limit point $(\mathbf{y}^*, \mathbf{X}^*, \mathbf{Z}^*)$ of the sequence $(\mathbf{y}^k, \mathbf{X}^k, \mathbf{Z}^k)$ generated by RWSADMM satisfies $\mathbf{y}^* = \mathbf{x}_i^*$, $i = 1, \dots, n$ where \mathbf{y}^* is a stationary point of Eq. (7), with probability 1, that is,

$$\Pr\left(0 \in \frac{1}{n} \sum_{i=1}^n \nabla f_i(\mathbf{y}^*)\right) = 1 \quad (27)$$

If the objective function of Eq. (7) is convex, then \mathbf{y}^* is a minimizer.

Next, Theorem 4.9 further presents that the algorithm converges sublinearly. This is comparable to the convergence rate of other FL methods [3, 2, 52, 64], but the existing methods didn't consider the dynamic graph and infrastructure-less environment. The detailed proof is offered in Appendix C.

Theorem 4.9. Under Assumptions (3.1), (4.1), and (4.2), with given β in Lemma 4.7, and local variables initiated as $\nabla f_i(\mathbf{x}_i^0) = \beta \mathbf{x}_i^0 = \mathbf{z}_i^0, \forall i \in \{1, \dots, n\}$, there exists a sequence $\{g^k\}_{k \geq 0}$ with $\{g^k\} \in \partial L_\beta^{k+1}$ satisfying

$$\min_{k \leq K} \mathbb{E} \|g^k\|^2 \leq \frac{C}{K} (L_\beta^0 - f), \quad \forall K > \tau(\delta) + 2 \quad (28)$$

where C is a constant depending on β, L , and γ, n , and $\tau(\delta)$.

Communication Complexity Using Theorem 4.9, the communication complexity of RWSADMM for nonconvex nonsmooth problems is as follows. To achieve ergodic gradient deviation

$E_t := \min_{k \leq K} \mathbb{E} \|g^k\|^2 \leq \omega$ for any $K > \tau(\delta) + 2$, it is sufficient to have

$$\frac{C}{K}(L_\beta^0 - f) \leq \omega \xrightarrow{(a)} K \sim O\left(\frac{1}{\omega} \cdot \frac{\tau(\delta)^2 + 1}{(1 - \delta)n\pi_*}\right) \quad (29)$$

(a) is achieved by taking L_β^0 and f as constants and independent of n and the network structure. Using the $\tau(\delta)$ definition from (6), by setting $\delta = 1/2$ and assuming the reversible Markov chain with $P(k)^T = P(k)$, the communication complexity is

$$O\left(\frac{1}{\omega} \cdot \frac{\ln^2 n}{(1 - \lambda_2(\mathbf{P}(k)))^2}\right) \quad (30)$$

Communication Comparison Among the baseline frameworks, Per-FedAvg [20] and APFL [64] have addressed the communication complexity of their respective frameworks. By assuming that Assumption 3.1 holds and utilizing Eq. (30), we can determine the communication complexity of RWSADMM as $O(\omega^{-1})$ for K iterations. In comparison, Per-FedAvg exhibits a higher communication complexity of $O(\omega^{-3/2})$. In the case of APFL, all clients are assumed to be used in each computation round to ensure convergence in nonconvex settings. The communication complexity of APFL is determined as $O(n^{3/4}\omega^{-3/4})$, where n represents the total number of clients. Consequently, when n is large, APFL exhibits a significantly higher communication rate than RWSADMM. Overall, the communication complexity analysis suggests that RWSADMM offers superior scalability and communication efficiency compared to existing methods.

5 Experimental Results

Setup We evaluate the performance of RWSADMM using heterogeneous data distributions. All the experiments are conducted on a workstation with Threadripper Pro 5955WX, 64GB DDR4 RAM, and NVidia 4090 GPU. All frameworks are performed on standard FL benchmark datasets (MNIST [50], Synthetic [19], and CIFAR10 [49]) with 10-class labels and convex and non-convex models. Multinomial logistic regression (MLR), multilayer perceptron network (MLP), and convolutional neural network (CNN) models are utilized for strongly convex and two non-convex settings, respectively. We create a moderately dynamic connected graph of randomly placed nodes where each node has at least 5 neighboring nodes at k -th update. We set the probability transition matrix $\mathbf{P}(k)$ as $[\mathbf{P}(k)]_{ij} = 1/\text{deg}(i_k)$ and set up the experiments for $N = 20$ clients with a regeneration frequency of 10 steps for the dynamic graph. The data is split among clients using a pathological non-IID setting. The data on each client contains a portion of labels (two out of ten labels), and the allocated data size for each client is variable. For the Synthetic data, we use the same data generative procedures of [19] with 60 features and 100 clients. All local datasets are split randomly with 75% and 25% for training and testing, respectively. The models’ details, the rationale behind graph construction, and hyperparameter tuning for β , κ , and selected ε value are further described in Appendix D.

Performance Comparison The performance of RWSADMM is compared with FedAvg [43] as a benchmark and several state-of-the-art personalized FL algorithms such as Per-FedAvg [20], pFedMe [19], APFL [64], and Ditto [52]. The test accuracy and training loss for the MNIST dataset is depicted in Fig. 2. (Synthetic and CIFAR10 figures are presented in Appendix D). Test accuracy and time cost for all the datasets are reported in Table 1.

The test accuracy progress curves of RWSADMM for all the models (2a-2c) have a significantly faster convergence. For the non-convex models (2b), RWSADMM reaches convergence after 200 iterations, while the rest of the algorithms, except Ditto, work toward convergence until 600 iterations. The performance curves are shown for 100 iterations for consistency. When tested on MNIST with MLP, RWSADMM demonstrated comparable performance against pFedMe. In the test on Synthetic data with MLR models, RWSADMM exhibited a significant advantage over the other methods, with an improved margin of 14.95%. Regarding computational efficiency, RWSADMM is slower than FedAvg and Per-FedAvg, but faster than pFedMe. Furthermore, RWSADMM converges in fewer iterations (200 iterations) than pFedMe (600 iterations). RWSADMM is also run for more extensive networks with 50 and 100 nodes as a separate set of experiments. The performance comparison results and diagrams are also in Appendix D.

6 Conclusion and Future Work

This study proposes a novel approach called RWSADMM, designed for systems with isolated nodes connected via wireless links to the mobile server without relying on pre-existing communication

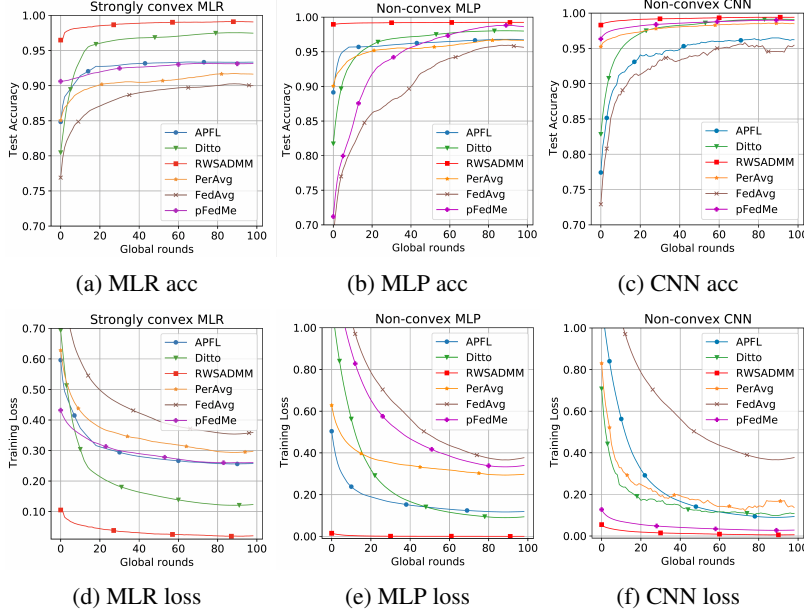


Figure 2: Performance comparison (test accuracy and training loss) of RWSADMM, pFedMe, Per-Avg, FedAvg, APFL, and Ditto for MNIST dataset for the MLR (2a, 2d), MLP (2b, 2e), and CNN (2c, 2f) models. The first 100 iterations are plotted to show the convergence progress better.

Frameworks	MNIST						Synthetic			
	MLR		MLP		CNN		MLR		MLP	
	acc(%)	t(s)	acc(%)	t(s)	acc(%)	t(s)	acc(%)	t(s)	acc(%)	t(s)
FedAvg	93.96 ± 0.02	384	98.79 ± 0.03	464	97.83 ± 0.15	7965	77.62 ± 0.11	592	83.64 ± 0.22	680
PerAvg	94.37 ± 0.04	472	98.90 ± 0.02	608	98.97 ± 0.08	7296	81.49 ± 0.09	800	85.01 ± 0.10	808
pFedMe	95.62 ± 0.04	1344	99.46 ± 0.01	2096	99.05 ± 0.06	16623	83.20 ± 0.06	760	86.36 ± 0.15	4240
Ditto	97.37 ± 0.02	828	97.79 ± 0.03	1268	99.20 ± 0.11	9820	86.24 ± 0.03	216	85.26 ± 0.10	236
APFL	92.64 ± 0.03	913	97.74 ± 0.02	1598	98.58 ± 0.03	17800	83.40 ± 0.04	284	82.52 ± 0.15	332
RWSADMM (our method)	98.63 ± 0.01	500	99.29 ± 0.02	884	99.52 ± 0.04	11570	96.44 ± 0.12	1420	97.17 ± 0.18	2076

Frameworks	CIFAR10					
	MLR		MLP		CNN	
	acc(%)	t(s)	acc(%)	t(s)	acc(%)	t(s)
FedAvg	40.84 ± 0.01	480	41.02 ± 0.05	205	38.65 ± 0.05	235
PerAvg	47.43 ± 0.09	576	60.25 ± 0.07	760	83.52 ± 0.01	2401
pFedMe	67.53 ± 0.34	1544	78.12 ± 0.38	1020	83.56 ± 0.05	10440
Ditto	75.2 ± 0.01	675	81.37 ± 0.13	778	83.86 ± 0.02	6566
APFL	75.17 ± 0.32	150	78.00 ± 0.18	165	66.23 ± 0.03	2106
RWSADMM (our method)	80.72 ± 0.11	392	84.99 ± 0.20	760	87.08 ± 0.03	11276

Table 1: Performance comparisons of FedAvg, Per-FedAvg, pFedMe, Ditto, APFL, and RWSADMM frameworks on MNIST, Synthetic, and CIFAR10 datasets. Three models are utilized for each dataset, and each model’s converged accuracy (%) and time consumption (seconds) are reported. Each configuration is executed for ten iterations, and variance is calculated to compute the degree of confidence for test accuracy rates.

infrastructure. The algorithm enables the server to move randomly toward a local client, establishing local proximity among adjacent clients based on hard inequality constraints, addressing the challenge of data heterogeneity. Theoretical and experimental results demonstrate that RWSADMM is fast-converging and communication-efficient, surpassing current state-of-the-art FL frameworks. This study primarily focuses on the methodological framework for RWSADMM. Future research directions should explore essential techniques such as incorporating differential privacy techniques and examining scalability in more extensive network and dataset scenarios. Further investigation is needed to assess the implementation in physical networks and evaluate the effect of communication delays in the real world.

References

- [1] Jia Hu, Tiande Guo, and Congying Han. Stochastic linearized generalized alternating direction method of multipliers: Expected convergence rates and large deviation properties. *Mathematical Structures in Computer Science*, pages 1–18, 2023.
- [2] Hao Yu, Sen Yang, and Shenghuo Zhu. Parallel restarted sgd with faster convergence and less communication: Demystifying why model averaging works for deep learning. In *Proceedings of the AAAI Conference on Artificial Intelligence*, volume 33, pages 5693–5700, 2019.
- [3] Sai Praneeth Karimireddy, Satyen Kale, Mehryar Mohri, Sashank Reddi, Sebastian Stich, and Ananda Theertha Suresh. Scaffold: Stochastic controlled averaging for federated learning. In *International Conference on Machine Learning*, pages 5132–5143. PMLR, 2020.
- [4] J Michael Gilmore. Warfighter information network–tactical (win-t) increment 2. 2015.
- [5] David A Handelman, Corban G Rivera, Robert St Amant, Emma A Holmes, Andrew R Badger, and Bryanna Y Yeh. Adaptive human-robot teaming through integrated symbolic and subsymbolic artificial intelligence: preliminary results. In *Artificial Intelligence and Machine Learning for Multi-Domain Operations Applications IV*, volume 12113, pages 145–157. SPIE, 2022.
- [6] Fal Sadikin and Sandeep Kumar. Zigbee iot intrusion detection system: A hybrid approach with rule-based and machine learning anomaly detection. In *IoTBDS*, pages 57–68, 2020.
- [7] Kang Wei, Jun Li, Ming Ding, Chuan Ma, Howard H Yang, Farhad Farokhi, Shi Jin, Tony QS Quek, and H Vincent Poor. Federated learning with differential privacy: Algorithms and performance analysis. *IEEE Transactions on Information Forensics and Security*, 15:3454–3469, 2020.
- [8] Minseok Ryu and Kibaek Kim. Differentially private federated learning via inexact admm. *arXiv preprint arXiv:2106.06127*, 2021.
- [9] Sheng Yue, Ju Ren, Jiang Xin, Sen Lin, and Junshan Zhang. Inexact-admm based federated meta-learning for fast and continual edge learning. In *Proceedings of the Twenty-second International Symposium on Theory, Algorithmic Foundations, and Protocol Design for Mobile Networks and Mobile Computing*, pages 91–100, 2021.
- [10] Qunwei Li, Bhavya Kailkhura, Ryan Goldhahn, Priyadip Ray, and Pramod K Varshney. Robust federated learning using admm in the presence of data falsifying byzantines. *arXiv preprint arXiv:1710.05241*, 2017.
- [11] Chaouki Ben Issaid, Anis Elgabri, Jihong Park, Mehdi Bennis, and Mérouane Debbah. Communication efficient distributed learning with censored, quantized, and generalized group admm. *arXiv preprint arXiv:2009.06459*, 2020.
- [12] Anis Elgabri, Jihong Park, Sabbir Ahmed, and Mehdi Bennis. L-fgadmm: Layer-wise federated group admm for communication efficient decentralized deep learning. In *2020 IEEE Wireless Communications and Networking Conference (WCNC)*, pages 1–6. IEEE, 2020.
- [13] Zonghao Huang, Rui Hu, Yuanxiong Guo, Eric Chan-Tin, and Yanmin Gong. Dp-admm: Admm-based distributed learning with differential privacy. *IEEE Transactions on Information Forensics and Security*, 15:1002–1012, 2019.
- [14] Peter Graf, Jennifer Annoni, Christopher Bay, Dave Biagioni, Devon Sigler, Monte Lunacek, and Wesley Jones. Distributed reinforcement learning with admm-rl. In *2019 American Control Conference (ACC)*, pages 4159–4166. IEEE, 2019.
- [15] Zijie Zheng, Lingyang Song, Zhu Han, Geoffrey Ye Li, and H Vincent Poor. A stackelberg game approach to proactive caching in large-scale mobile edge networks. *IEEE Transactions on Wireless Communications*, 17(8):5198–5211, 2018.
- [16] Xueru Zhang, Mohammad Mahdi Khalili, and Mingyan Liu. Improving the privacy and accuracy of admm-based distributed algorithms. In *International Conference on Machine Learning*, pages 5796–5805. PMLR, 2018.
- [17] Changkyu Song, Sejong Yoon, and Vladimir Pavlovic. Fast admm algorithm for distributed optimization with adaptive penalty. In *Proceedings of the AAAI Conference on Artificial Intelligence*, volume 30:1, 2016.

- [18] Stephen Boyd, Neal Parikh, Eric Chu, Borja Peleato, Jonathan Eckstein, et al. Distributed optimization and statistical learning via the alternating direction method of multipliers. *Foundations and Trends® in Machine Learning*, 3(1):1–122, 2011.
- [19] Canh T Dinh, Nguyen Tran, and Josh Nguyen. Personalized federated learning with moreau envelopes. *Advances in Neural Information Processing Systems*, 33:21394–21405, 2020.
- [20] Alireza Fallah, Aryan Mokhtari, and Asuman Ozdaglar. Personalized federated learning with theoretical guarantees: A model-agnostic meta-learning approach. *Advances in Neural Information Processing Systems*, 33:3557–3568, 2020.
- [21] Yihan Jiang, Jakub Konečný, Keith Rush, and Sreeram Kannan. Improving federated learning personalization via model agnostic meta learning. *arXiv preprint arXiv:1909.12488*, 2019.
- [22] Alex Nichol and John Schulman. Reptile: a scalable metalearning algorithm. *arXiv preprint arXiv:1803.02999*, 2(3):4, 2018.
- [23] Yishay Mansour, Mehryar Mohri, Jae Ro, and Ananda Theertha Suresh. Three approaches for personalization with applications to federated learning. *arXiv preprint arXiv:2002.10619*, 2020.
- [24] Peter Kairouz, H Brendan McMahan, Brendan Avent, Aurélien Bellet, Mehdi Bennis, Arjun Nitin Bhagoji, Kallista Bonawitz, Zachary Charles, Graham Cormode, Rachel Cummings, et al. Advances and open problems in federated learning. *Foundations and Trends® in Machine Learning*, 14(1–2):1–210, 2021.
- [25] Rui Hu, Yuanxiong Guo, Hongning Li, Qingqi Pei, and Yanmin Gong. Personalized federated learning with differential privacy. *IEEE Internet of Things Journal*, 7(10):9530–9539, 2020.
- [26] Manoj Ghuhana Arivazhagan, Vinay Aggarwal, Aaditya Kumar Singh, and Sunav Choudhary. Federated learning with personalization layers. *arXiv preprint arXiv:1912.00818*, 2019.
- [27] Jeffrey Li, Mikhail Khodak, Sebastian Caldas, and Ameet Talwalkar. Differentially private meta-learning. *arXiv preprint arXiv:1909.05830*, 2019.
- [28] Virginia Smith, Chao-Kai Chiang, Maziar Sanjabi, and Ameet S Talwalkar. Federated multi-task learning. *Advances in neural information processing systems*, 30, 2017.
- [29] Tian Li, Anit Kumar Sahu, Ameet Talwalkar, and Virginia Smith. Federated learning: Challenges, methods, and future directions. *IEEE Signal Processing Magazine*, 37(3):50–60, 2020.
- [30] Wei Yang Bryan Lim, Nguyen Cong Luong, Dinh Thai Hoang, Yutao Jiao, Ying-Chang Liang, Qiang Yang, Dusit Niyato, and Chunyan Miao. Federated learning in mobile edge networks: A comprehensive survey. *IEEE Communications Surveys & Tutorials*, 22(3):2031–2063, 2020.
- [31] Syreen Banabilah, Moayad Aloqaily, Eitaa Alsayed, Nida Malik, and Yaser Jararweh. Federated learning review: Fundamentals, enabling technologies, and future applications. *Information Processing & Management*, 59(6):103061, 2022.
- [32] S Sundhar Ram, A Nedić, and Venugopal V Veeravalli. Incremental stochastic subgradient algorithms for convex optimization. *SIAM Journal on Optimization*, 20(2):691–717, 2009.
- [33] Tao Sun, Yuejiao Sun, and Wotao Yin. On markov chain gradient descent. *Advances in neural information processing systems*, 31, 2018.
- [34] Suhail M Shah and Konstantin E Avrachenkov. Linearly convergent asynchronous distributed admm via markov sampling. *arXiv preprint arXiv:1810.05067*, 2018.
- [35] Xianghui Mao, Kun Yuan, Yubin Hu, Yuantao Gu, Ali H Sayed, and Wotao Yin. Walkman: A communication-efficient random-walk algorithm for decentralized optimization. *IEEE Transactions on Signal Processing*, 68:2513–2528, 2020.
- [36] Kai Lai Chung and Paul Erdos. On the application of the borel-cantelli lemma. *Transactions of the American Mathematical Society*, 72(1):179–186, 1952.
- [37] Xiaoyu Li and Francesco Orabona. On the convergence of stochastic gradient descent with adaptive stepsizes. In *The 22nd international conference on artificial intelligence and statistics*, pages 983–992. PMLR, 2019.
- [38] Xingyu Zhou. On the fenchel duality between strong convexity and lipschitz continuous gradient. *arXiv preprint arXiv:1803.06573*, 2018.

- [39] Yaliang Li, Bolin Ding, and Jingren Zhou. A practical introduction to federated learning. In *Proceedings of the 28th ACM SIGKDD Conference on Knowledge Discovery and Data Mining*, pages 4802–4803, 2022.
- [40] Dylan Mäenpää. Towards peer-to-peer federated learning: Algorithms and comparisons to centralized federated learning, 2021.
- [41] Dinh C Nguyen, Ming Ding, Pubudu N Pathirana, Aruna Seneviratne, Jun Li, and H Vincent Poor. Federated learning for internet of things: A comprehensive survey. *IEEE Communications Surveys & Tutorials*, 23(3):1622–1658, 2021.
- [42] Sashank Reddi, Zachary Charles, Manzil Zaheer, Zachary Garrett, Keith Rush, Jakub Konečný, Sanjiv Kumar, and H Brendan McMahan. Adaptive federated optimization. *arXiv preprint arXiv:2003.00295*, 2020.
- [43] Brendan McMahan, Eider Moore, Daniel Ramage, Seth Hampson, and Blaise Aguera y Arcas. Communication-efficient learning of deep networks from decentralized data. In *Artificial intelligence and statistics*, pages 1273–1282. PMLR, 2017.
- [44] Wei Shi, Qing Ling, Kun Yuan, Gang Wu, and Wotao Yin. On the linear convergence of the admm in decentralized consensus optimization. *IEEE Transactions on Signal Processing*, 62(7):1750–1761, 2014.
- [45] Shenglong Zhou and Geoffrey Ye Li. Federated learning via inexact admm. *arXiv preprint arXiv:2204.10607*, 2022.
- [46] Angelia Nedic, Alex Olshevsky, Asuman Ozdaglar, and John N Tsitsiklis. Distributed subgradient methods and quantization effects. In *2008 47th IEEE conference on decision and control*, pages 4177–4184. IEEE, 2008.
- [47] Ohad Shamir and Tong Zhang. Stochastic gradient descent for non-smooth optimization: Convergence results and optimal averaging schemes. In *International conference on machine learning*, pages 71–79. PMLR, 2013.
- [48] Kenta Niwa, Guoqiang Zhang, W Bastiaan Kleijn, Noboru Harada, Hiroshi Sawada, and Akinori Fujino. Asynchronous decentralized optimization with implicit stochastic variance reduction. In *International Conference on Machine Learning*, pages 8195–8204. PMLR, 2021.
- [49] Alex Krizhevsky, Geoffrey Hinton, et al. Learning multiple layers of features from tiny images. *Citeseer*, 2009.
- [50] Yann LeCun. The mnist database of handwritten digits. <http://yann.lecun.com/exdb/mnist/>, 1998.
- [51] R Tyrrell Rockafellar and Roger J-B Wets. *Variational analysis*, volume 317. Springer Science & Business Media, 2009.
- [52] Tian Li, Shengyuan Hu, Ahmad Beirami, and Virginia Smith. Ditto: Fair and robust federated learning through personalization. In *International Conference on Machine Learning*, pages 6357–6368. PMLR, 2021.
- [53] Karan Singhal, Hakim Sidahmed, Zachary Garrett, Shanshan Wu, John Rush, and Sushant Prakash. Federated reconstruction: Partially local federated learning. *Advances in Neural Information Processing Systems*, 34:11220–11232, 2021.
- [54] Xiaohan Liu, Tao Yang, and Baoping Yan. Internet of things for wildlife monitoring. In *2015 IEEE/CIC International Conference on Communications in China-Workshops (CIC/ICCC)*, pages 62–66. IEEE, 2015.
- [55] Viktor Toldov, Laurent Clavier, and Nathalie Mitton. Multi-channel distributed mac protocol for wsn-based wildlife monitoring. In *2018 14th International Conference on Wireless and Mobile Computing, Networking and Communications (WiMob)*, pages 1–8. IEEE, 2018.
- [56] Bilal Arshad, Johan Barthelemy, Elliott Pilton, and Pascal Perez. Where is my deer?-wildlife tracking and counting via edge computing and deep learning. In *2020 IEEE SENSORS*, pages 1–4. IEEE, 2020.
- [57] Nancy Victor, Mamoun Alazab, Sweta Bhattacharya, Sindri Magnusson, Praveen Kumar Reddy Maddikunta, Kadiyala Ramana, Thippa Reddy Gadekallu, et al. Federated learning for iout: Concepts, applications, challenges and opportunities. *arXiv preprint arXiv:2207.13976*, 2022.

- [58] Chien-Chi Kao, Yi-Shan Lin, Geng-De Wu, and Chun-Ju Huang. A comprehensive study on the internet of underwater things: applications, challenges, and channel models. *Sensors*, 17(7):1477, 2017.
- [59] Lulwa Ahmed, Kashif Ahmad, Naina Said, Basheer Qolomany, Junaid Qadir, and Ala Al-Fuqaha. Active learning based federated learning for waste and natural disaster image classification. *IEEE Access*, 8:208518–208531, 2020.
- [60] Ahmed Imteaj, Irfan Khan, Javad Khazaei, and Mohammad Hadi Amini. Fedresilience: A federated learning application to improve resilience of resource-constrained critical infrastructures. *Electronics*, 10(16):1917, 2021.
- [61] Nishat I Mowla, Nguyen H Tran, Inshil Doh, and Kijoon Chae. Federated learning-based cognitive detection of jamming attack in flying ad-hoc network. *IEEE Access*, 8:4338–4350, 2019.
- [62] Beibei Li, Yukun Jiang, Wenbin Sun, Weina Niu, and Peiran Wang. Fedvanet: Efficient federated learning with non-iid data for vehicular ad hoc networks. In *2021 IEEE Global Communications Conference (GLOBECOM)*, pages 1–6. IEEE, 2021.
- [63] Hideya Ochiai, Yuwei Sun, Qingzhe Jin, Nattanon Wongwiwatchai, and Hiroshi Esaki. Wireless ad hoc federated learning: A fully distributed cooperative machine learning. *arXiv preprint arXiv:2205.11779*, 2022.
- [64] Yuyang Deng, Mohammad Mahdi Kamani, and Mehrdad Mahdavi. Adaptive personalized federated learning. *arXiv preprint arXiv:2003.13461*, 2020.
- [65] Dirk Helbing and Evangelos Pournaras. Society: Build digital democracy. *Nature*, 527(7576):33–34, 2015.
- [66] Amit Kumar Bairwa and Sandeep Joshi. Mla-rpm: A machine learning approach to enhance trust for secure routing protocol in mobile ad hoc networks. *Int J Adv Sci Technol*, 29(04):11265–11274, 2020.
- [67] Mingyi Hong, Davood Hajinezhad, and Ming-Min Zhao. Prox-pda: The proximal primal-dual algorithm for fast distributed nonconvex optimization and learning over networks. In *International Conference on Machine Learning*, pages 1529–1538. PMLR, 2017.
- [68] John Gastil and Robert C Richards. Embracing digital democracy: A call for building an online civic commons. *PS: Political Science & Politics*, 50(3):758–763, 2017.
- [69] Sebastian U Stich. Local sgd converges fast and communicates little. *arXiv preprint arXiv:1805.09767*, 2018.
- [70] Farzin Haddadpour and Mehrdad Mahdavi. On the convergence of local descent methods in federated learning. *arXiv preprint arXiv:1910.14425*, 2019.

A RWSADMM: Algorithm

The RWSADMM scheme is as presented in Algorithm 1. Client i_k is selected by Random Walk via $P(k)$, and \mathbf{y}'_{i_k} is the token from the previous update. Note that we only use one client in each derivation iteration. Still, it is straightforward to generalize the algorithm to have multiple active clients in $\mathcal{S}(i_k) \subset \mathcal{N}(i_k)$ simultaneously to stabilize the computation better as follows:

$$\mathbf{y}_{i_k} = \mathbf{y}'_{i_k} + \frac{1}{n_{i_k} S_{i_k}} \sum_{i_k \in \mathcal{S}(i_k)} [\mathbf{x}_{i_k} - (\frac{\mathbf{z}_{i_k}}{\beta} + \boldsymbol{\varepsilon}_{i_k}) \odot \text{sgn}(\mathbf{t}_{i_k})] - \sum_{i_k \in \mathcal{S}(i_k)} [\mathbf{x}'_{i_k} - (\frac{\mathbf{z}'_{i_k}}{\beta} + \boldsymbol{\varepsilon}_{i_k}) \odot \text{sgn}(\mathbf{t}'_{i_k})] \quad (31)$$

where S_{i_k} represents the volume of $\mathcal{S}(i_k)$.

Algorithm 1 RWSADMM

1: **Initialization:**

Initialize Markov transition matrices $\{\mathbf{P}(0), \mathbf{P}(1), \dots\}$.

Initialize $\{\mathbf{x}_i^0\}_{i=1}^n = 0$, $\{\mathbf{z}_i^0\}_{i=1}^n = 0$, and

$$\mathbf{y}^1 = \frac{1}{n} \sum_{i=1}^n (\mathbf{x}_i^0 - \frac{\mathbf{z}_i^0}{\beta}) = 0 \quad (32)$$

2: **RWSADMM**(β, \mathbf{y}_1):

3: **repeat**

4: **for** $k \in 0, 1, 2, \dots$ **do**

5: Client i_k receives \mathbf{y}'_{i_k} and updates \mathbf{X} , \mathbf{Z} , and \mathbf{y} using equations (11), (15), and (14);

6: **end for**

$\kappa = 0.99 \times \kappa$

7: **until** the termination condition is TRUE.

RETURN $\mathbf{X}^*, \mathbf{y}^*$

B RWSADMM: Convergence Analysis

Our proof of convergence for the proposed stochastic ADMM-based federated learning algorithm is non-trivial and non-straightforward. It introduces novel techniques to address the challenge of integrating the mobilized server and stochasticity into our federated ADMM framework. Specifically, we carefully consider the movement of the server, which is realized by using a dynamic Markov matrix. This is a significant novelty and challenge in the proof, as it is the first method introduced in federated learning that considers this type of server movement. By introducing assumptions on the dynamic Markov matrix and accounting for the dynamic behavior of the server, we are able to guarantee the convergence of our algorithm under certain conditions. While there are a few existing works, such as [1] that address convergence rates and properties of LADMM algorithms, they are not directly applicable to our random walk mobilization and stochastic update setting and are not directly adaptable to the unique requirements of federated learning. As such, our work represents a significant contribution to the field and provides valuable insights into the convergence properties of stochastic ADMM-based federated learning algorithms. We believe that our novel approach and careful consideration of the movement of the server will inspire further research and development in this area, leading to more effective and efficient federated learning algorithms. The proof sketch of the Convergence Theorem (Theorem 4.8) is as follows.

Proof. The proof sketch is summarized as follows.

1. Under Assumption 4.2, the sequence created by the RWSADMM, i.e., $(\mathbf{y}^k, \mathbf{X}^k, \mathbf{Z}^k)_{k > T}$,

satisfies $\|\mathbf{Z}^{k+1} - \mathbf{Z}^k\| = \sum \|\mathbf{z}_{i_k}^{k+1} - \mathbf{z}_{i_k}^k\| \leq L \|\mathbf{X}^{\tau(k, i_k)+1} - \mathbf{X}^{\tau(k, i_k)}\|$

2. Recall L_β^k defined in Eq. (25). For $k \geq 0$, the RWSADMM iterates satisfy

$$L_\beta^k - L_\beta (\mathbf{y}^{k+1}, \mathbf{X}^k; \mathbf{Z}^k) \geq \|\mathbf{y}^k - \mathbf{y}^{k+1}\|^2$$

3. Under Assumption 4.2, for $\beta > L$ and $\forall k > T$,

$$L_\beta (\mathbf{y}^{k+1}, \mathbf{X}^k; \mathbf{Z}^k) - L_\beta^{k+1} \geq \frac{\beta - L}{2n} \|\mathbf{X}^k - \mathbf{X}^{k+1}\|^2 - \frac{L^2}{n\beta} \|\mathbf{X}^{\tau(k, i_k)+1} - \mathbf{X}^{\tau(k, i_k)}\|^2$$

4. Recall M_β^k defined in Eq. (25); under Assumption 4.2, for $\beta > 2L^2 + L + 2$ and $\forall k > T$,

$$M_\beta^k - M_\beta^{k+1} \geq \frac{\beta}{2} \|\mathbf{y}^k - \mathbf{y}^{k+1}\|^2 + \frac{1}{n} \|\mathbf{X}^k - \mathbf{X}^{k+1}\|^2 + \frac{L^2}{2n} \|\mathbf{X}^{\tau(k, i_k)+1} - \mathbf{X}^{\tau(k, i_k)}\|^2 \quad (33)$$

5. For $\beta > 2L^2 + L + 2$, RWSADMM ensures a lower bounded sequence $(M_\beta^k)_{k \geq 0}$.

□

The proof details are provided in the following. Several steps are taken to prove Lemma 4.7. We introduce several Lemmas to represent these steps (Lemma B.1-B.5). Lemma B.1 shows that the update of the primal variable can bound the update on the dual variable.

Lemma B.1. Under Assumption 4.2, the sequence created by RWSADMM, $(\mathbf{y}^k, \mathbf{X}^k, \mathbf{Z}^k)_{k > T}$, satisfies,

$$\mathbb{E} \left\| \mathbf{Z}^{k+1} - \mathbf{Z}^k \right\| = \mathbb{E} \left\| \mathbf{z}_{i_k}^{k+1} - \mathbf{z}_{i_k}^k \right\| \leq L \cdot \mathbb{E} \left\| \mathbf{X}^{\tau(k, i_k)+1} - \mathbf{X}^{\tau(k, i_k)} \right\| \quad (34)$$

Proof. Note that client i_k is activated at iteration k . Denote \mathbf{x}_i^k , \mathbf{z}_i^k , and \mathbf{x}_i^k as the three groups of variables owned by any client i ($1 \leq \forall i \leq n$) at iteration k . Under the Assumption 4.4, the optimality condition of \mathbf{X} update for $i = i_k$ implies that

$$\mathbb{E}_\xi [\text{sgn}(\mathbf{t}') (g_i(\mathbf{x}_i^k, \xi) + \boldsymbol{\varepsilon}_i^k - \mathbf{z}_i^k) + \beta(\mathbf{y}^{k+1} - \mathbf{x}_{i_k}^{k+1})] = 0 \quad (35)$$

Substituting Eq. (35) into Eq. (15) yields

$$\mathbb{E}_\xi [g_i(\mathbf{x}_i^k, \xi)] = \mathbb{E}_\xi [\mathbf{z}_{i_k}^{k+1}], \text{ for } i = i_k \quad (36)$$

Hence, for $i = i_k$, we have

$$\begin{aligned} \mathbb{E} \left\| \mathbf{z}_i^{k+1} - \mathbf{z}_i^k \right\| &\stackrel{(a)}{=} \mathbb{E} \left\| \mathbf{z}_i^{k+1} - \mathbf{z}_i^{\tau(k, i)+1} \right\| \stackrel{(36)}{=} \left\| \mathbb{E}_\xi (g_i(\mathbf{x}_i^k, \xi) + \boldsymbol{\varepsilon}_i^{k+1}) - \mathbb{E}_\xi (g_i(\mathbf{x}_i^{\tau(k, i)}, \xi) + \boldsymbol{\varepsilon}_i^k) \right\| \\ &\stackrel{(b)}{=} \left\| \mathbb{E}_\xi (g_i(\mathbf{x}_i^{\tau(k, i)+1}, \xi)) - \mathbb{E}_\xi (g_i(\mathbf{x}_i^{\tau(k, i)}, \xi)) \right\| \stackrel{(17\&20)}{\leq} L \cdot \mathbb{E}_\xi \left\| \mathbf{x}_i^{\tau(k, i)+1} - \mathbf{x}_i^{\tau(k, i)} \right\| \end{aligned} \quad (37)$$

where $\tau(k, i)$ is defined in Eq. (24). The equality (a) holds because $\mathbf{z}_i^k = \mathbf{z}_i^{\tau(k, i)+1}$, and equality (b) holds because $\mathbf{x}_i^k = \mathbf{x}_i^{\tau(k, i)+1}$. On the other hand, when $i \neq i_k$, agent i is not activated at iteration k , so $\mathbb{E}_\xi [\|\mathbf{z}_{i_k}^{k+1} - \mathbf{z}_{i_k}^k\|] = L \mathbb{E}_\xi [\|\mathbf{x}_{i_k}^{k+1} - \mathbf{x}_{i_k}^k\|] = 0$. Therefore, we have the proof of Eq. (34). □

Lemma B.2 shows that the \mathbf{y} -update in RWSADMM provides a sufficient descent of the augmented Lagrangian.

Lemma B.2. Recall L_β^k defined in Eq. (25). For $k \geq 0$, RWSADMM iterates satisfies

$$L_\beta^k - L_\beta \left(\mathbf{y}^{k+1}, \mathbf{X}^k; \mathbf{Z}^k \right) \geq \|\mathbf{y}^k - \mathbf{y}^{k+1}\|^2 \quad (38)$$

Proof. We rewrite the augmented Lagrangian function L in Eq. (8) by adding and subtracting the term $\|\mathbf{Z}\|^2/2\beta$ to the RHS of the equation and rearranging the terms. One can obtain

$$L_\beta(\mathbf{Y}, \mathbf{X}; \mathbf{Z}) = \frac{1}{n} \left(F(\mathbf{X}) + \frac{\beta}{2} \left\| \mathbf{1} \otimes \mathbf{y} - \mathbf{X} \right\| - \epsilon + \frac{\mathbf{Z}}{\beta} \right)^2 - \frac{\|\mathbf{Z}\|^2}{2\beta} \quad (39)$$

So, the augmented Lagrangian update is

$$\begin{aligned}
L_\beta^k - L_\beta(\mathbf{y}^{k+1}, \mathbf{X}^k; \mathbf{Z}^k) &= \frac{\beta}{2n} \left\| \mathbf{1} \otimes \mathbf{y}^k - \mathbf{X}^k - \boldsymbol{\epsilon}^k + \frac{\mathbf{Z}^k}{\beta} \right\|^2 - \frac{\beta}{2n} \left\| \mathbf{1} \otimes \mathbf{y}^{k+1} - \mathbf{X}^k - \boldsymbol{\epsilon}^k + \frac{\mathbf{Z}^k}{\beta} \right\|^2 \\
&\stackrel{(a)}{=} \frac{\beta}{2n} \sum_{i=1}^n \left(\|\mathbf{y}^k - \mathbf{y}^{k+1}\|^2 + 2 \left\langle |\mathbf{y}^{k+1} - \mathbf{x}_i^k| - \boldsymbol{\epsilon}^k + \frac{\mathbf{z}_i^k}{\beta}, \mathbf{y}^k - \mathbf{y}^{k+1} \right\rangle \right) \geq \frac{\beta}{2} \|\mathbf{y}^k - \mathbf{y}^{k+1}\|^2 - \langle \mathbf{d}^k, \mathbf{y}^k - \mathbf{y}^{k+1} \rangle
\end{aligned} \tag{40}$$

The equality (a) is achieved by applying the cosine identity $\|b + c\|^2 - \|a + c\|^2 = \|b - a\|^2 + 2 \langle a + c, b - a \rangle$, and \mathbf{d}^k is defined as

$$\mathbf{d}^k := -\frac{\beta}{n} \sum_{i=1}^n \left(|\mathbf{y}^{k+1} - \mathbf{x}_i^k| - \boldsymbol{\epsilon}^k + \frac{\mathbf{z}_i^k}{\beta} \right) = 0 \tag{41}$$

which results from \mathbf{y} -update in the RWSADMM algorithm. \square

In Lemma B.3, the lower bound of descent in the augmented Lagrangian over the updates of \mathbf{X} and \mathbf{Z} is derived.

Lemma B.3. Recall L_β^k defined in Eq. 25. Under Assumption 4.2, for $\beta > L$ and $\forall k > T$,

$$\mathbb{E}[L_\beta(\mathbf{y}^{k+1}, \mathbf{X}^k; \mathbf{Z}^k) - L_\beta^{k+1}] \geq \frac{\gamma - L}{2n} \mathbb{E} \left\| \mathbf{X}^k - \mathbf{X}^{k+1} \right\|^2 - \frac{L^2}{n\beta} \mathbb{E} \left\| \mathbf{X}^{\tau(k, i_k)+1} - \mathbf{X}^{\tau(k, i_k)} \right\|^2 \tag{42}$$

Proof. For the augmented Lagrangian L_β , we derive

$$\begin{aligned}
& L_\beta(\mathbf{y}^{k+1}, \mathbf{X}^k; \mathbf{Z}^k) - L_\beta^{k+1} \\
&= \frac{1}{n}(f_{i_k}(\mathbf{x}_{i_k}^k) + \langle \mathbf{z}_{i_k}^k, |\mathbf{y}^{k+1} - \mathbf{x}_{i_k}^k| - \boldsymbol{\varepsilon}_{i_k}^k \rangle) + \frac{\beta}{2} \|\mathbf{y}^{k+1} - \mathbf{x}_{i_k}^k| - \boldsymbol{\varepsilon}_{i_k}^k\|^2 \\
&\quad - f_{i_k}(\mathbf{x}_{i_k}^{k+1}) - \langle \mathbf{z}_{i_k}^{k+1}, |\mathbf{y}^{k+1} - \mathbf{x}_{i_k}^{k+1}| - \boldsymbol{\varepsilon}_{i_k}^k \rangle - \frac{\beta}{2} \|\mathbf{y}^{k+1} - \mathbf{x}_{i_k}^{k+1}| - \boldsymbol{\varepsilon}_{i_k}^k\|^2 \\
&= \frac{1}{n}(f_{i_k}(\mathbf{x}_{i_k}^k) - \langle \mathbf{z}_{i_k}^{k+1}, |\mathbf{y}^{k+1} - \mathbf{x}_{i_k}^{k+1}| - \boldsymbol{\varepsilon}_{i_k}^k \rangle - f_{i_k}(\mathbf{x}_{i_k}^{k+1})) \\
&\quad + \langle \mathbf{z}_{i_k}^k, |\mathbf{y}^{k+1} - \mathbf{x}_{i_k}^k| - \boldsymbol{\varepsilon}_{i_k}^k \rangle - \frac{\beta}{2} \left[\|\mathbf{y}^{k+1} - \mathbf{x}_{i_k}^{k+1}| - \boldsymbol{\varepsilon}_{i_k}^k\|^2 - \|\mathbf{y}^{k+1} - \mathbf{x}_{i_k}^k| - \boldsymbol{\varepsilon}_{i_k}^k\|^2 \right] \\
&\stackrel{(a)}{=} \frac{1}{n}(f_{i_k}(\mathbf{x}_{i_k}^k) - \langle \mathbf{z}_{i_k}^{k+1}, |\mathbf{y}^{k+1} - \mathbf{x}_{i_k}^{k+1}| - \boldsymbol{\varepsilon}_{i_k}^k \rangle - f_{i_k}(\mathbf{x}_{i_k}^{k+1}) + \langle \mathbf{z}_{i_k}^k, |\mathbf{y}^{k+1} - \mathbf{x}_{i_k}^k| - \boldsymbol{\varepsilon}_{i_k}^k \rangle) \\
&\quad - \frac{\beta}{2} \left[\|\mathbf{x}_{i_k}^{k+1} - \mathbf{x}_{i_k}^k\|^2 + 2 \langle |\mathbf{y}^{k+1} - \mathbf{x}_{i_k}^{k+1}| - \boldsymbol{\varepsilon}_{i_k}^k, \mathbf{x}_{i_k}^{k+1} - \mathbf{x}_{i_k}^k \rangle \right] \\
&= \frac{1}{n}(f_{i_k}(\mathbf{x}_{i_k}^k) - \langle \mathbf{z}_{i_k}^{k+1}, |\mathbf{y}^{k+1} - \mathbf{x}_{i_k}^{k+1}| - \boldsymbol{\varepsilon}_{i_k}^k \rangle - f_{i_k}(\mathbf{x}_{i_k}^{k+1})) \\
&\quad + \langle \mathbf{z}_{i_k}^k, |\mathbf{y}^{k+1} - \mathbf{x}_{i_k}^k| - \boldsymbol{\varepsilon}_{i_k}^k \rangle - \frac{\beta}{2} \|\mathbf{x}_{i_k}^{k+1} - \mathbf{x}_{i_k}^k\|^2 \\
&\quad - \beta \langle |\mathbf{y}^{k+1} - \mathbf{x}_{i_k}^{k+1}| - \boldsymbol{\varepsilon}_{i_k}^k, \mathbf{x}_{i_k}^{k+1} - \mathbf{x}_{i_k}^k \rangle \\
&\stackrel{(b)}{=} \frac{1}{n}(f_{i_k}(\mathbf{x}_{i_k}^k) - f_{i_k}(\mathbf{x}_{i_k}^{k+1})) + \left\langle \mathbf{z}_{i_k}^k, \frac{\mathbf{z}_{i_k}^{k+1} - \mathbf{z}_{i_k}^k}{\beta} + \mathbf{x}_{i_k}^{k+1} - \mathbf{x}_{i_k}^k \right\rangle - \frac{\beta}{2} \|\mathbf{x}_{i_k}^{k+1} - \mathbf{x}_{i_k}^k\|^2 \\
&\quad - \left\langle \mathbf{z}_{i_k}^{k+1}, \frac{\mathbf{z}_{i_k}^{k+1} - \mathbf{z}_{i_k}^k}{\beta} \right\rangle - \beta \left\langle \frac{\mathbf{z}_{i_k}^{k+1} - \mathbf{z}_{i_k}^k}{\beta}, \mathbf{x}_{i_k}^{k+1} - \mathbf{x}_{i_k}^k \right\rangle \\
&= \frac{1}{n}(f_{i_k}(\mathbf{x}_{i_k}^k) + \frac{\mathbf{z}_{i_k}^{k+1} \mathbf{z}_{i_k}^k}{\beta} - \frac{(\mathbf{z}_{i_k}^k)^2}{\beta} + \mathbf{z}_{i_k}^k (\mathbf{x}_{i_k}^{k+1} - \mathbf{x}_{i_k}^k) - f_{i_k}(\mathbf{x}_{i_k}^{k+1})) \\
&\quad + \frac{\beta}{2} \|\mathbf{x}_{i_k}^k - \mathbf{x}_{i_k}^{k+1}\|^2 - \frac{(\mathbf{z}_{i_k}^{k+1})^2}{\beta} + \frac{\mathbf{z}_{i_k}^{k+1} \mathbf{z}_{i_k}^k}{\beta} - (\mathbf{z}_{i_k}^{k+1} - \mathbf{z}_{i_k}^k)(\mathbf{x}_{i_k}^k - \mathbf{x}_{i_k}^{k+1})) \\
&= \frac{1}{n}(f_{i_k}(\mathbf{x}_{i_k}^k) - f_{i_k}(\mathbf{x}_{i_k}^{k+1})) - \frac{1}{\beta} (\mathbf{z}_{i_k}^k)^2 + (\mathbf{z}_{i_k}^{k+1})^2 - 2(\mathbf{z}_{i_k}^{k+1} \mathbf{z}_{i_k}^k) \\
&\quad + \frac{\beta}{2} \|\mathbf{x}_{i_k}^k - \mathbf{x}_{i_k}^{k+1}\|^2 - \mathbf{z}_{i_k}^{k+1} (\mathbf{x}_{i_k}^k - \mathbf{x}_{i_k}^{k+1}) \\
&\stackrel{(c)}{=} \frac{1}{n}(f_{i_k}(\mathbf{x}_{i_k}^k) + \frac{\beta}{2} \|\mathbf{x}_{i_k}^k - \mathbf{x}_{i_k}^{k+1}\|^2 - f_{i_k}(\mathbf{x}_{i_k}^{k+1})) - \frac{1}{\beta} \|\mathbf{z}_{i_k}^{k+1} - \mathbf{z}_{i_k}^k\|^2 - \langle \mathbf{z}_{i_k}^{k+1}, \mathbf{x}_{i_k}^k - \mathbf{x}_{i_k}^{k+1} \rangle
\end{aligned} \tag{43}$$

Where equality (a) holds due to the cosine identity $\|b + c\|^2 - \|a + c\|^2 = \|b - a\|^2 + 2 \langle b - a, c \rangle$, equality (b) holds because of \mathbf{y} -update in RWSADMM, and equality (c) holds due to recursion of \mathbf{y} -update in RWSADMM. Next, we apply the stochastic property to Eq. (43) using Eq. (36),

$$\begin{aligned}
& \mathbb{E}[L_\beta(\mathbf{y}^{k+1}, \mathbf{X}^k; \mathbf{Z}^k) - L_\beta^{k+1}] \\
&= \frac{1}{n} (\mathbb{E}_\xi [f_{i_k}(\mathbf{x}_{i_k}^k) - f_{i_k}(\mathbf{x}_{i_k}^{k+1})] - \langle E_\xi (g_i(\mathbf{x}_i^k, \xi) + \epsilon^k), \mathbf{x}_{i_k}^k - \mathbf{x}_{i_k}^{k+1} \rangle \\
&+ \frac{\beta}{2} E_\xi \|\mathbf{x}_{i_k}^k - \mathbf{x}_{i_k}^{k+1}\|^2 - \frac{1}{\beta} \mathbb{E}_\xi \|\mathbf{z}_{i_k}^{k+1} - \mathbf{z}_{i_k}^k\|^2) \\
&\stackrel{(a)}{\geq} \frac{1}{n} \left(-\frac{L}{2} \mathbb{E}_\xi \|\mathbf{x}_{i_k}^k - \mathbf{x}_{i_k}^{k+1}\|^2 + \frac{\beta}{2} \mathbb{E}_\xi \|\mathbf{x}_{i_k}^k - \mathbf{x}_{i_k}^{k+1}\|^2 - \frac{1}{\beta} \mathbb{E}_\xi \|\mathbf{z}_{i_k}^{k+1} - \mathbf{z}_{i_k}^k\|^2 \right) \quad (44) \\
&\stackrel{(b)}{\geq} \frac{1}{n} \left(-\frac{L}{2} \mathbb{E}_\xi \|\mathbf{x}_{i_k}^k - \mathbf{x}_{i_k}^{k+1}\|^2 + \frac{\beta}{2} \mathbb{E}_\xi \|\mathbf{x}_{i_k}^k - \mathbf{x}_{i_k}^{k+1}\|^2 - \frac{L^2}{\beta} \mathbb{E}_\xi \|\mathbf{x}_{i_k}^{\tau(k, i_k)+1} - \mathbf{x}_{i_k}^{\tau(k, i_k)}\|^2 \right) \\
&= \frac{\beta - L}{2n} \mathbb{E}_\xi \|\mathbf{x}_{i_k}^k - \mathbf{x}_{i_k}^{k+1}\|^2 - \frac{L^2}{n\beta} \mathbb{E}_\xi \|\mathbf{x}_{i_k}^{\tau(k, i_k)+1} - \mathbf{x}_{i_k}^{\tau(k, i_k)}\|^2
\end{aligned}$$

Where inequality (a) is achieved using Assumption 4.2 (Eq. (18)), and inequality (b) is due to Lemma B.1 (Eq. (34)). \square

In Lemma B.4, the sufficient descent in Lyapunov functions is established.

Lemma B.4. Recall M_β^k defined in Eq. (25); under Assumption 4.2, for $\beta > 2L^2 + L + 2$ and $\forall k > T$,

$$M_\beta^k - M_\beta^{k+1} \geq \frac{\beta}{2} \|\mathbf{y}^k - \mathbf{y}^{k+1}\|^2 + \frac{1}{n} \|\mathbf{X}^k - \mathbf{X}^{k+1}\|^2 + \frac{L^2}{2n} \|\mathbf{X}^{\tau(k, i_k)+1} - \mathbf{X}^{\tau(k, i_k)}\|^2 \quad (45)$$

Proof. Using Eq. (25), we can attain

$$\begin{aligned}
& M_\beta^k - M_\beta^{k+1} \\
&= L_\beta^k - L_\beta^{k+1} + \frac{L^2}{n} \left(\|\mathbf{x}_i^{\tau(k, i_k)+1} - \mathbf{x}_i^{\tau(k, i_k)}\|^2 - \|\mathbf{x}_i^{\tau(k+1, i_k)+1} - \mathbf{x}_i^{\tau(k+1, i_k)}\|^2 \right) \\
&\stackrel{(a)}{=} L_\beta^k - L_\beta^{k+1} + \frac{L^2}{n} \left(\|\mathbf{x}_{i_k}^{\tau(k, i_k)+1} - \mathbf{x}_{i_k}^{\tau(k, i_k)}\|^2 - \|\mathbf{x}_{i_k}^{k+1} - \mathbf{x}_{i_k}^k\|^2 \right) \quad (46) \\
&= L_\beta^k - L_\beta^{k+1} + \frac{L^2}{n} \left(\|\mathbf{X}^{\tau(k, i_k)+1} - \mathbf{X}^{\tau(k, i_k)}\|^2 - \|\mathbf{X}^{k+1} - \mathbf{X}^k\|^2 \right)
\end{aligned}$$

where inequality (a) is due to the following property,

$$x_i^{\tau(k+1, i)+1} - x_i^{\tau(k+1, i)} = \begin{cases} x_i^{k+1} - x_i^k, & i = i_k \\ x_i^{\tau(k, i)+1} - x_i^{\tau(k, i)}, & \text{otherwise} \end{cases} \quad (47)$$

Substituting Eq. (33), one can obtain

$$M_\beta^k - M_\beta^{k+1} \geq L_\beta(\mathbf{y}^{k+1}, \mathbf{X}^k; \mathbf{Z}^k) - L_\beta^{k+1} + \|\mathbf{y}^k - \mathbf{y}^{k+1}\|^2 + \frac{L^2}{n} \left(\|\mathbf{X}^{\tau(k, i_k)+1} - \mathbf{X}^{\tau(k, i_k)}\|^2 - \|\mathbf{X}^{k+1} - \mathbf{X}^k\|^2 \right) \quad (48)$$

One can also substitute Eq. (33) into Eq. (48), which leads to

$$\begin{aligned}
& M_\beta^k - M_\beta^{k+1} \\
&\geq \frac{\beta - L}{2n} \|\mathbf{X}^k - \mathbf{X}^{k+1}\|^2 - \frac{L^2}{n\beta} \|\mathbf{X}^{\tau(k, i_k)+1} - \mathbf{X}^{\tau(k, i_k)}\|^2 \\
&+ \|\mathbf{y}^k - \mathbf{y}^{k+1}\|^2 + \frac{L^2}{n} \left(\|\mathbf{X}^{\tau(k, i_k)+1} - \mathbf{X}^{\tau(k, i_k)}\|^2 - \|\mathbf{X}^{k+1} - \mathbf{X}^k\|^2 \right) \quad (49) \\
&= \frac{\beta - L - 2L^2}{2n} \|\mathbf{X}^k - \mathbf{X}^{k+1}\|^2 + \frac{L^2(\beta - 1)}{n\beta} \|\mathbf{X}^{\tau(k, i_k)+1} - \mathbf{X}^{\tau(k, i_k)}\|^2 + \|\mathbf{y}^k - \mathbf{y}^{k+1}\|^2
\end{aligned}$$

Using $\frac{\beta}{2} - \frac{L}{2} - L^2 \geq 1$, $1 - \frac{1}{\beta} > \frac{1}{2}$, and $\beta < 2$, we complete the proof of Eq. (45). \square

Lemma B.5 states that the Lyapunov function M_β^k is lower bounded.

Lemma B.5. For $\beta > 2L^2 + L + 2$, RWSADMM ensures a lower bounded sequence $(M_\beta^k)_{k \geq 0}$ in expectation.

Proof. For $k > T$, we have

$$\begin{aligned}
& \mathbb{E}[M_\beta^k] \\
&= \mathbb{E}[L_\beta^k] + \frac{L^2}{n} \sum_{i=1}^n \mathbb{E} \left\| \mathbf{x}_i^{\tau(k, i_k)+1} - \mathbf{x}_i^{\tau(k, i_k)} \right\|^2 \\
&= \frac{1}{n} \sum_{j=1}^n \mathbb{E} \left(f_j(\mathbf{x}_j^k) + \langle \mathbf{z}_j^k, |\mathbf{y}^k - \mathbf{x}_j^k| - \boldsymbol{\varepsilon}_j^k \rangle \right) + \frac{\beta}{2n} \sum_{j=1}^n \mathbb{E} \left\| \mathbf{y}_j^k - \mathbf{X}_j^k \right\|^2 \\
&+ \frac{L^2}{n} \sum_{i=1}^n \mathbb{E} \left\| \mathbf{x}_i^{\tau(k, i_k)+1} - \mathbf{x}_i^{\tau(k, i_k)} \right\|^2 \\
&\stackrel{(a)}{=} \frac{1}{n} \sum_{j=1}^n \mathbb{E} \left(f_j(\mathbf{x}_j^k) + \langle \mathbb{E}_\xi(g_j(\mathbf{x}_j^{\tau(k, j)}, \xi)), \mathbf{y}^k - \mathbf{x}_j^k \rangle \right) + \frac{\beta}{2n} \sum_{j=1}^n \mathbb{E} \left\| \mathbf{y}_j^k - \mathbf{X}_j^k \right\|^2 + \frac{L^2}{n} \sum_{i=1}^n \mathbb{E} \left\| \mathbf{x}_i^k - \mathbf{x}_i^{\tau(k, i_k)} \right\|^2 \\
&\stackrel{(b)}{\geq} \frac{1}{n} \sum_{j=1}^n \mathbb{E} \left(f_j(\mathbf{y}^k) + \langle \mathbb{E}_\xi(g_j(\mathbf{x}_j^{\tau(k, j)}, \xi)) - \mathbb{E}_\xi(g_j(\mathbf{x}_i^k, \xi)), \mathbf{y}^k - \mathbf{x}_j^k \rangle \right) \\
&+ \frac{\beta - L}{2n} \sum_{j=1}^n \mathbb{E} \left\| \mathbf{y}_j^k - \mathbf{X}_j^k \right\|^2 + \frac{L^2}{n} \sum_{i=1}^n \mathbb{E} \left\| \mathbf{x}_i^k - \mathbf{x}_i^{\tau(k, i_k)} \right\|^2 \\
&\stackrel{(c)}{\geq} \frac{1}{n} \sum_{j=1}^n \mathbb{E} \left(f_j(\mathbf{y}^k) + \left\| \mathbb{E}_\xi(g_j(\mathbf{x}_i^{\tau(k, j)}, \xi)) - \mathbb{E}_\xi(g_j(\mathbf{x}_i^k, \xi)) \right\|^2 \right) \\
&+ \frac{\beta - L - 2}{2n} \mathbb{E} \left\| \mathbf{1} \otimes \mathbf{y}^k - \mathbf{X}^k \right\|^2 + \frac{L^2}{n} \sum_{i=1}^n \mathbb{E} \left\| \mathbf{x}_i^k - \mathbf{x}_i^{\tau(k, i_k)} \right\|^2 \\
&\stackrel{(d)}{\geq} \min_{\mathbf{y}} \left\{ \frac{1}{n} \sum_{j=1}^n \mathbb{E} f_j(\mathbf{y}^k) \right\} + \frac{2L^2}{2n} \mathbb{E} \left\| \mathbf{1} \otimes \mathbf{y}^k - \mathbf{X}^k \right\|^2 \\
&\stackrel{(e)}{\geq} -\infty
\end{aligned} \tag{50}$$

where (a) holds due to Eq. (36). (b) holds because f_j is Lipschitz differentiable (Eq. (22)). (c) holds due to Young's inequality. (d) follows from the assumption $\beta > 2L^2 + L + 2$ and the Lipschitz smoothness of each f_j , and (e) holds due to Assumption 4.1. Therefore, M_β^k is bounded from below in expectation. \square

Now we can prove Lemma 4.7 with the above lemmas.

Proof. Recall that the maximum hitting time T is almost surely finite. For Statement 1, the monotonicity of Lyapunov function $(M_\beta^k)_{k > T}$ in Lemma B.4 and their lower boundedness in Lemma B.5 ensure convergence of $(M_\beta^k)_{k \geq 0}$. For Statement 2, consider Statement 1 and the lower boundedness of $(M_\beta^k)_{k > T}$ in Lemma B.5 (Eq. (50)). $\frac{1}{n} F(\mathbf{y}^k)$ is upper bounded by $\max\{\max_{t \in \{0, \dots, T\}} \frac{1}{n} F(\mathbf{y}^t), M_\beta^{T+1}\}$; and $\left\| \mathbf{1} \otimes \mathbf{y}_j^k - \mathbf{X}_j^k \right\|^2$ is upper bounded by $\max\{\max_{t \in \{0, \dots, T\}} \left\| \mathbf{1} \otimes \mathbf{y}_j^t - \mathbf{X}_j^t \right\|^2, L_\beta^{T+1}\}$. By Assumption 4.1, the sequence $\{\mathbf{y}^k | k = \{0, 1, \dots\}\}$ is bounded. The boundedness of $\left\| \mathbf{1} \otimes \mathbf{y}_j^k - \mathbf{X}_j^k \right\|^2$ further leads to that of $\{\mathbf{X}_j^k | k = \{0, 1, \dots\}\}$. Finally, Eq. (36) and Assumption 4.2 ensure (\mathbf{Z}^k) is bounded as well. Altogether, $(\mathbf{y}^k, \mathbf{X}^k, \mathbf{Z}^k)$ is bounded. \square

Based on Lemma 4.7, the convergence of the subgradients of L_β^k can be established as follows.

Lemma B.6. With Assumption 4.5 and β given in Lemma 4.7, for any given subsequence (including the whole sequence) with its index $(k_s)_{s \geq 0}$, there exists a sequence $(g^k)_{k \geq 0}$ with $(g^k) \in \partial L_\beta^{k+1}$ containing an almost surely convergent subsequence $(g^{k_{s_j}})_{j \geq 0}$, that is,

$$Pr \left(\lim_{j \rightarrow \infty} \left\| g^{k_{s_j}} = 0 \right\| \right) = 1$$

Proof. The proof sketch is summarized as follows.

1. We construct the sequence $g^k \in \partial L_\beta^{k+1}$ and show that its subvector $q_i^k := (g_{\mathbf{y}^i}^k, g_{\mathbf{x}^i}^k, g_{\mathbf{z}^i}^k)$ satisfies $\lim_{k \rightarrow \infty} \mathbb{E} \left\| q_{i_k}^{k-\tau(\delta)-1} \right\|^2 = 0$, where the mixing time $\tau(\delta)$ is defined in Eq. (6).
2. For $k \geq 0$, define the filtration of sigma algebras:
 $\chi^k = \sigma(\mathbf{y}^0, \dots, \mathbf{y}^k, \mathbf{X}^0, \dots, \mathbf{X}^k, \mathbf{Z}^0, \dots, \mathbf{Z}^k, i_0, \dots, i_k)$. We show that

$$\mathbb{E} \left(\left\| q_{i_k}^{k-\tau(\delta)-1} \right\|^2 \middle| \chi^{k-\tau(\delta)} \right) \geq (1-\delta) \pi_* \left\| g^{k-\tau(\delta)-1} \right\|^2,$$
where π_* is the minimal value in the Markov chain's stationary distribution. From this bound and the result in Step 1, we can get $\lim_{k \rightarrow \infty} \left\| g^k \right\| = 0$.
3. From the result in Step 2, we use the Borel-Cantelli lemma [36] to obtain an almost unquestionably convergent subsubsequence of g^k .

□

The details of these steps are given as follows.

Proof. First, recall Lemma B.4 and $T < \infty$, we have

$$\sum_{k=0}^{\infty} \left(\mathbb{E} \left\| \mathbf{y}^k - \mathbf{y}^{k+1} \right\|^2 + \mathbb{E} \left\| \mathbf{X}^k - \mathbf{X}^{k+1} \right\|^2 + \mathbb{E} \left\| \mathbf{X}^{\tau(k, i_k)} - \mathbf{X}^{\tau(k, i_k)+1} \right\|^2 \right) < +\infty \quad (51)$$

Hence, by Lemma B.4, one can infer

$$\sum_{k=0}^{\infty} \left(\mathbb{E} \left\| \mathbf{y}^k - \mathbf{y}^{k+1} \right\|^2 + \mathbb{E} \left\| \mathbf{X}^k - \mathbf{X}^{k+1} \right\|^2 + \mathbb{E} \left\| \mathbf{Z}^k - \mathbf{Z}^{k+1} \right\|_2^2 \right) < +\infty \quad (52)$$

Step 1: The proof starts with computing the subgradients of the augmented Lagrangian Eq. (39) with the updates in RWSADMM,

$$\frac{\partial L_\beta^{k+1}}{\partial \mathbf{y}} \ni -\frac{\beta}{n} (\mathbf{x}_{i_k}^{k+1} - \mathbf{x}_{i_k}^k) + \frac{1}{n} (\mathbf{z}_{i_k}^{k+1} - \mathbf{z}_{i_k}^k) =: w^k \quad (53)$$

$$\nabla_{\mathbf{x}_j} L_\beta^{k+1} = \frac{1}{n} \left(\nabla f_j(\mathbf{x}_j^{k+1}) - \mathbf{z}_j^{k+1} + \beta(\mathbf{x}_j^{k+1} - \mathbf{y}^{k+1}) \right) \quad (54)$$

$$\nabla_{\mathbf{z}_j} L_\beta^{k+1} = \frac{1}{n} (\mathbf{y}^{k+1} - \mathbf{x}_j^{k+1}) \quad (55)$$

We define g^k and q_i^k as

$$g^k := \begin{bmatrix} w^k \\ \nabla_{\mathbf{X}} L_\beta^{k+1} \\ \nabla_{\mathbf{Z}} L_\beta^{k+1} \end{bmatrix}, q_i^k := \begin{bmatrix} w^k \\ \nabla_{\mathbf{x}_i} L_\beta^{k+1} \\ \nabla_{\mathbf{z}_i} L_\beta^{k+1} \end{bmatrix} \quad (56)$$

where $i \in \mathbf{V}$ is the index of the agent and g^k is the gradient of L_k^β . For $\delta \in (0, 1)$ and $k \geq \tau(\delta) + 1$,

$$\left\| q_{i_k}^{k-\tau(\delta)-1} \right\|^2 = \left\| q_{i_k}^{k-\tau(\delta)-1} - q_{i_k}^k + q_{i_k}^k \right\|^2 \stackrel{(a)}{\leq} 2 \underbrace{\left\| q_{i_k}^{k-\tau(\delta)-1} - q_{i_k}^k \right\|^2}_A + 2 \underbrace{\left\| q_{i_k}^k \right\|^2}_B \quad (57)$$

We upper bound A and B separately. A has three parts corresponding to the three parts of g . Its first part is

$$\begin{aligned} & \left\| w^{k-\tau(\delta)-1} - w^k \right\|^2 \\ & \leq 2 \left\| w^{k-\tau(\delta)-1} \right\|^2 + 2 \left\| w^k \right\|^2 \\ & \stackrel{(53)}{\leq} \frac{4}{n^2} \left(\beta^2 \left\| \mathbf{X}^{k+1} - \mathbf{X}^k \right\|^2 + \beta^2 \left\| \mathbf{X}^{k-\tau(\delta)} - \mathbf{X}^{k-\tau(\delta)-1} \right\|^2 \right) \\ & \quad + \left\| \mathbf{Z}^{k+1} - \mathbf{Z}^k \right\|^2 + \left\| \mathbf{Z}^{k-\tau(\delta)} - \mathbf{Z}^{k-\tau(\delta)-1} \right\|^2 \end{aligned} \quad (58)$$

Then by Eq. (54), we bound the 2nd part of A

$$\begin{aligned} & \left\| \nabla_{\mathbf{x}_{i_k}} L_\beta^{k-\tau(\delta)-1} - \nabla_{\mathbf{x}_{i_k}} L_\beta^{k+1} \right\|^2 \\ & \stackrel{(a)}{\leq} \frac{4L^2 + 4\beta^2}{n^2} \left\| \mathbf{x}_{i_k}^{k-\tau(\delta)-1} - \mathbf{x}_{i_k}^{k+1} \right\|^2 + \frac{4}{n^2} \left\| \mathbf{z}_{i_k}^{k-\tau(\delta)-1} - \mathbf{z}_{i_k}^{k+1} \right\|^2 \\ & \quad + \frac{4\beta^2}{n^2} \left\| \mathbf{y}^{k-\tau(\delta)-1} - \mathbf{y}^{k+1} \right\|^2 \\ & \leq \frac{D}{n^2} \sum_{t=k-\tau(\delta)-1}^k \left(\left\| \mathbf{y}^t - \mathbf{y}^{t+1} \right\|^2 + \left\| \mathbf{X}^t - \mathbf{X}^{t+1} \right\|^2 + \left\| \mathbf{Z}^t - \mathbf{Z}^{t+1} \right\|^2 \right) \end{aligned} \quad (59)$$

where $D = (\tau(\delta) + 2)(4 + 4\beta^2 + 4L^2)$, and (a) uses the inequality of arithmetic and geometric means and Lipschitz differentiability of f_j in Assumption 4.2. From Eq. (55). The third part of A can be bounded as

$$\begin{aligned} & \left\| \nabla_{\mathbf{z}_{i_k}} L_\beta^{k-\tau(\delta)-1} - \nabla_{\mathbf{z}_{i_k}} L_\beta^{k+1} \right\|^2 \\ & \leq \frac{2}{n^2} \left(\left\| \mathbf{y}^{k-\tau(\delta)-1} - \mathbf{y}^{k+1} \right\|^2 + \left\| \mathbf{x}_{i_k}^{k-\tau(\delta)-1} - \mathbf{x}_{i_k}^{k+1} \right\|^2 \right) \\ & \leq \frac{2(\tau(\delta) + 2)}{n^2} \sum_{t=k-\tau(\delta)-1}^k \left(\left\| \mathbf{y}^t - \mathbf{y}^{t+1} \right\|^2 + \left\| \mathbf{X}^t - \mathbf{X}^{t+1} \right\|^2 \right) \end{aligned} \quad (60)$$

Plugging Eq. (58), Eq. (59), and Eq. (60) into term A, we get a constant $C_1 \sim O\left(\frac{\tau(\delta)+1}{n^2}\right)$, depending on $\tau(\delta)$, β , L , and n , such that

$$A \leq C_1 \sum_{t=k-\tau(\delta)-1}^k \left(\left\| \mathbf{y}^t - \mathbf{y}^{t+1} \right\|^2 + \left\| \mathbf{x}^t - \mathbf{x}^{t+1} \right\|^2 + \left\| \mathbf{z}^t - \mathbf{z}^{t+1} \right\|^2 \right) \quad (61)$$

To bound the term B, using Eq. (55) and \mathbf{Z} -update (Eq. (15)), we have

$$\nabla_{\mathbf{z}_{i_k}} L_\beta^{k+1} = \frac{1}{n\beta} (\mathbf{z}_{i_k}^{k+1} - \mathbf{z}_{i_k}^k) \quad (62)$$

Applying Eq. (54) and Eq. (36), we drive $\nabla_{\mathbf{x}_{i_k}} L_\beta^{k+1}$:

$$\nabla_{\mathbf{x}_{i_k}} L_\beta^{k+1} = \frac{1}{n\beta} \left(\nabla f_{i_k}(\mathbf{x}_{i_k}^{k+1}) - \nabla f_{i_k}(\mathbf{x}_{i_k}^k) + \mathbf{z}_{i_k}^k - \mathbf{z}_{i_k}^{k+1} \right) \quad (63)$$

So we have

$$B \leq C_2 (\|\mathbf{x}^t - \mathbf{x}^{t+1}\|^2 + \|\mathbf{z}^t - \mathbf{z}^{t+1}\|^2) \quad (64)$$

for a constant C_2 depending on L , β , and n , in the order of $O(\frac{1}{n^2})$. Then substituting Eq. (61) and Eq. (64) into Eq. (57) and taking expectations, it yields

$$\begin{aligned} & \mathbb{E} \left\| q_{i_k}^{k-\tau(\delta)-1} \right\|^2 \\ & \leq C \sum_{t=k-\tau(\delta)-1}^k (\mathbb{E} \|\mathbf{y}^t - \mathbf{y}^{t+1}\|^2 + \mathbb{E} \|\mathbf{x}^t - \mathbf{x}^{t+1}\|^2 + \mathbb{E} \|\mathbf{z}^t - \mathbf{z}^{t+1}\|^2) \end{aligned} \quad (65)$$

where $C = C_1 + C_2$, and $C \sim O(\frac{\tau(\delta)+1}{n^2})$. Recalling Eq. (52), we get the convergence

$$\lim_{k \rightarrow \infty} \mathbb{E} \left\| q_{i_k}^{k-\tau(\delta)-1} \right\|^2 = 0 \quad (66)$$

which completes the proof of **Step 1**.

Step 2: We compute the expectation:

$$\begin{aligned} & \mathbb{E} \left(\left\| q_{i_k}^{k-\tau(\delta)-1} \right\|^2 \chi^{k-\tau(\delta)} \right) \\ & = \sum_{j=1}^n [\mathbf{P}(k)^{\tau(\delta)}]_{i_{k-\tau(\delta)}, j} (\left\| \nabla_{\mathbf{y}} L_{\beta}^{k-\tau(\delta)} \right\|^2 + \left\| \nabla_{\mathbf{x}_j} L_{\beta}^{k-\tau(\delta)} \right\|^2) \\ & \quad + \left\| \nabla_{\mathbf{z}_j} L_{\beta}^{k-\tau(\delta)} \right\|^2 \stackrel{(a)}{\geq} (1-\delta) \pi_* \left\| g^{k-\tau(\delta)-1} \right\|^2 \end{aligned} \quad (67)$$

where (a) follows from Eq. (4) and the definition of g_k in Eq. (56). Then, with Eq. (65), one can derive

$$\lim_{k \rightarrow \infty} \mathbb{E} \|g^k\|^2 = \lim_{k \rightarrow \infty} \mathbb{E} \left\| g^{k-\tau(\delta)-1} \right\|^2 = 0, \quad (68)$$

By the Schwarz inequality $(\mathbb{E} \|g^k\|)^2 \leq \mathbb{E} \|g^k\|^2$, we have

$$\lim_{k \rightarrow \infty} \mathbb{E} \|g^k\| = 0, \quad (69)$$

Step 3: By Markov's inequality, for each $\omega > 0$, it holds that

$$Pr(\|g_k\| > \omega) \leq \frac{\mathbb{E} \|g^k\|}{\omega} \stackrel{Eq.(68)}{\xrightarrow{k \rightarrow \infty}} \lim_{k \rightarrow \infty} Pr(\|g_k\| > \omega) = 0 \quad (70)$$

when a subsequence $(k_s)_{s \geq 0}$ is provided, Eq. (69) implies,

$$Pr(\|g_{k_s}\| > \omega) = 0 \quad (71)$$

Then, for $j \in \mathbb{N}$, select $\omega = 2^{-j}$ and we can find a nondecreasing subsubsequence (k_{s_j}) , such that

$$Pr(\|g_{k_{s_j}}\| > 2^{-j}) \leq 2^{-j}, \quad \forall k_{s_j} \geq k_{s_j} \quad (72)$$

We have

$$\sum_{j=1}^{\infty} Pr(\|g_{k_{s_j}}\| > 2^{-j}) \leq \sum_{j=1}^{\infty} 2^{-j} = 1 \quad (73)$$

The Borel-Cantelli lemma yields

$$Pr\left(\limsup_j \{\|g_{k_s}\| > 2^{-j}\}\right) = 0 \quad (74)$$

and thus

$$Pr\left(\lim_j \|g_{k_{s_j}}\| = 0\right) = 1 \quad (75)$$

This completes **Step 3** and thus the entire **Lemma B.6**. \square

Proof of Convergence Finally, we present the proof of the convergence theorem (Theorem 4.8) as follows.

Proof. By statement 2 of Lemma 4.7, the sequence $(\mathbf{y}^k, \mathbf{X}^k, \mathbf{Z}^k)$ is bounded, so there exists a convergent subsequence $(\mathbf{y}^{k_s}, \mathbf{X}^{k_s}, \mathbf{Z}^{k_s})$ converging to a limit point $(\mathbf{y}^*, \mathbf{X}^*, \mathbf{Z}^*)$ as $s \rightarrow \infty$. By continuity, we have

$$L_\beta(\mathbf{y}^*, \mathbf{X}^*, \mathbf{Z}^*) = \lim_{s \rightarrow \infty} L_\beta(\mathbf{y}^{k_s}, \mathbf{X}^{k_s}, \mathbf{Z}^{k_s}) \quad (76)$$

Lemma B.6 finds a subsubsequence $g^{k_{s_j}} \in \partial L_\beta^{k+1}$ such that $Pr(\lim_{j \rightarrow \infty} \|g^{k_{s_j}}\| = 0) = 1$. By the definition of general subgradient ([51], def 8.3), we have $0 \in \partial L_\beta(\mathbf{y}^*, \mathbf{X}^*, \mathbf{Z}^*)$. Hence, Theorem 4.8 is proved. \square

C RWSADMM: Convergence Rate Analysis

The detailed proof of the convergence rate theorem is as follows.

Proof. It can be verified that under specific initialization, Eq. (36) holds for all $k \geq 0$. Consequently, Lemmas B.1-B.4 hold for all $k \geq 0$. For g^k defined in Eq. (56), Eq. (65) and Eq. (67) hold. Jointly applying Eq. (65) and Eq. (67), for any $k > \tau(\delta) + 1$, one has

$$\begin{aligned} \mathbb{E}\|g^{k-\tau(\delta)-1}\|^2 &\leq \frac{C}{(1-\delta)\pi_*} \\ &\sum_{t=k-\tau(\delta)-1}^k (\mathbb{E}\|\mathbf{y}^t - \mathbf{y}^{t+1}\|^2 + \mathbb{E}\|\mathbf{X}^t - \mathbf{X}^{t+1}\|^2 + \mathbb{E}\|\mathbf{Z}^t - \mathbf{Z}^{t+1}\|^2) \end{aligned} \quad (77)$$

According to Lemmas B.1 and B.4, for $k \geq \tau(\delta) + 1$, it holds,

$$\begin{aligned} &\sum_{t=k-\tau(\delta)-1}^k (\mathbb{E}\|\mathbf{y}^t - \mathbf{y}^{t+1}\|^2 + \mathbb{E}\|\mathbf{X}^t - \mathbf{X}^{t+1}\|^2 + \mathbb{E}\|\mathbf{Z}^t - \mathbf{Z}^{t+1}\|^2) \\ &\leq \max\left\{\frac{2}{\beta-\gamma}, (1+L^2)n\right\} (\mathbb{E}L_\beta^{k-\tau(\delta)-1} - \mathbb{E}L_\beta^{k+1}) \end{aligned} \quad (78)$$

It implies that for any $k \geq 0$, it holds

$$\mathbb{E}\|g^k\|^2 \leq C' (\mathbb{E}L_\beta^k - \mathbb{E}L_\beta^{k+\tau(\delta)+2}) \quad (79)$$

where $C' := \max\left\{\frac{2}{\beta-\gamma}, (1+L^2)n\right\} \frac{C}{(1-\delta)\pi_*}$. It can be verified that $C' = O\left(\frac{\tau(\delta)+1}{(1-\delta)n\pi_*}\right)$. Let $\tau' := \tau(\delta) + 2$; for any $K > \tau'$, summing Eq. (79) over $k \in \{K - \tau', \dots, \text{mod}_{\tau'} K\}$ gives

$$\sum_{l=1}^{\lfloor \frac{K}{\tau'} \rfloor} \mathbb{E} \|g^{K-l\tau'}\|^2 \leq C' \left(\mathbb{E} L_{\beta}^{\text{mod}_{\tau'} K} - \mathbb{E} L_{\beta}^K \right) \leq C' (L_{\beta}^0 - \underline{f}) \quad (80)$$

where the last inequality follows from the non-decreasing property of the sequence $(L_{\beta}^k)_{k \geq 0}$ and the fact that $(L_{\beta}^k)_{k \geq 0}$ is lower bounded by \underline{f} . According to Eq. (80),

$$\begin{aligned} \min_{k \leq K} \mathbb{E} \|g^k\|^2 &\leq \min_{1 \leq l \leq \lfloor \frac{K}{\tau'} \rfloor} \mathbb{E} \|g^{K-l\tau'}\|^2 \\ &\leq \frac{1}{\lfloor \frac{K}{\tau'} \rfloor} \sum_{l=1}^{\lfloor \frac{K}{\tau'} \rfloor} \mathbb{E} \|g^{K-l\tau'}\|^2 \leq \frac{\tau' C'}{K - \tau'} (L_{\beta}^0 - \underline{f}) \\ &\leq \frac{C'(\tau' + 1)}{K} (L_{\beta}^0 - \underline{f}) \end{aligned} \quad (81)$$

where the constant $C'(\tau' + 1) = O\left(\frac{\tau(\delta)^2 + 1}{(1-\delta)n\pi_*}\right)$. \square

We consider a reversible Markov chain on an undirected graph. Using the definition of $\tau(\delta)$ in Eq. (6) and setting $\delta = 1/2$, one has $\tau(\delta) \sim \frac{\ln n}{1 - \lambda_2(P(k))}$. To guarantee $\min_{k \leq K} \mathbb{E} \|g^k\|^2 \leq \omega$, certain number of iterations is sufficient,

$$O\left(\frac{1}{\omega} \cdot \left(\frac{\ln^2 n}{(1 - \lambda_2(P(k)))^2}\right) + 1\right) \quad (82)$$

D Experiments

D.1 Models

One strongly convex model and two non-convex models are utilized in our implementations. An MLR model with a logistic regression classifier is implemented for the strongly convex setting. For the first non-convex setting, an MLP model with two hidden dense layers of vector image size (resizing the 2D image as 1D vector) and 100 hidden nodes in the hidden layer are implemented. The cross-entropy loss is employed for this network. For the second non-convex setting, a CNN model with two convolutional layers with convolution operations of size 5×5 and one fully-connected layer of 512 followed by a Softmax layer is implemented. The cross-entropy loss is utilized in the network, and dropout rates of 25% and 50% are applied after convolutional layers.

D.2 Graph Construction

To meet this requirement on Assumption 3.1, we propose using a Markov transition matrix \mathbf{P} with a maximum eigenvalue of less than $1 - 1/m^{2/3}$, where m is the number of edges. To fulfill this inequality, we can increase the number of edges in the network. In our experiments, we have addressed this issue by requiring each client to be a neighbor of at least M other clients, which ensures a sufficient number of edges to satisfy the assumption on \mathbf{P} . By incorporating this requirement into our implementation, we can guarantee the validity of our results and ensure that our algorithm performs optimally under realistic conditions.

D.3 Hyperparameter tuning

The two hyperparameters of RWSADMM (β and κ) must be fine-tuned to optimize the performance. In the first stage of the experiments, we set $\kappa = 0.001$ and search for the optimal values of β . The fine-tuning process is performed for each dataset and each model separately. In Fig. 3, the effect of β values on the performance of RWSADMM for the MNIST dataset is presented.

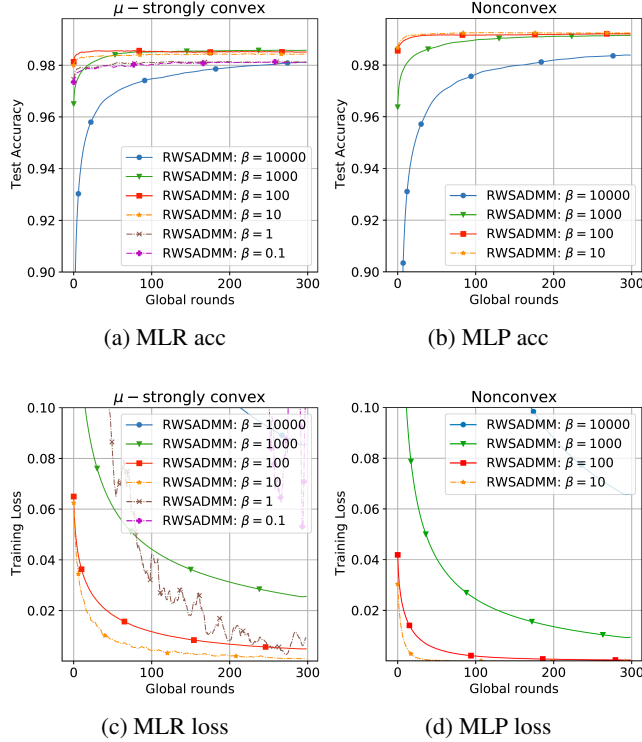


Figure 3: Effect of β on the convergence of RWSADMM in the MLR (3a, 3c) and MLP (3b, 3d) models for MNIST dataset.

The κ parameter, which affects the dual variable \mathbf{Z} , is also fine-tuned in the second stage. Same as the first stage, κ is fine-tuned for the MNIST dataset for the MLR, MLP, and CNN models, and the results are shown in Fig. 4. The optimal values of $\{\kappa = 0.001, 0.01\}$ have the best performances for MLR and MLP, respectively.

The proximal parameter, ϵ , is set to a fixed value of $\{\epsilon = 1e - 5\}$ for all the experiments. For the MNIST dataset, the fine-tuned parameter values of $\beta = 10$ and $\kappa = 0.001$ for MLR, $\beta = 10$ and $\kappa = 0.01$ for MLP are used. For the Synthetic dataset, $\beta = 10$ and $\kappa = 0.01$ for MLR, $\beta = 100$ and $\kappa = 0.01$ for MLP models are utilized. Finally, for CIFAR10 dataset, $\beta = 100$ and $\kappa = 0.001$ for MLR, $\beta = 100$ and $\kappa = 1$ for MLP are used.

D.4 CIFAR10 figures

The performance comparison of RWSADMM, FedAvg, Per-FedAvg, pFedMe, APFL, and Ditto for the Cifar10 dataset are depicted in Fig. 5. The fine-tuned values of $\beta = 0.001$ and $\kappa = 0.001$ are used for RWSADMM. The RWSADMM has a steep curve nearly reaching the optimal values from the first few rounds in strongly convex and non-convex models, indicating a faster convergence process than the benchmark algorithms. Also, RWSADMM shows a clear advantage for MLR or DNN models for accuracy.

D.5 Synthetic figures

Due to the 1D nature of the synthetic dataset, only MLR and MLP models are utilized for it. The performance comparison of RWSADMM, FedAvg, Per-FedAvg, pFedMe, APFL, and Ditto for the Synthetic dataset are depicted in Fig. 6. The fine-tuned values of $\beta = 100$ and $\kappa = 0.001$ are used for RWSADMM for all the settings. By comparing the accuracy and loss diagrams, RWSADMM performs visibly better than the rest of the algorithms in both strongly convex and non-convex settings. The accuracy rate of RWSADMM shows accuracy improvement compared with the benchmark algorithms by the margin of 14% for both MLR and MLP models.

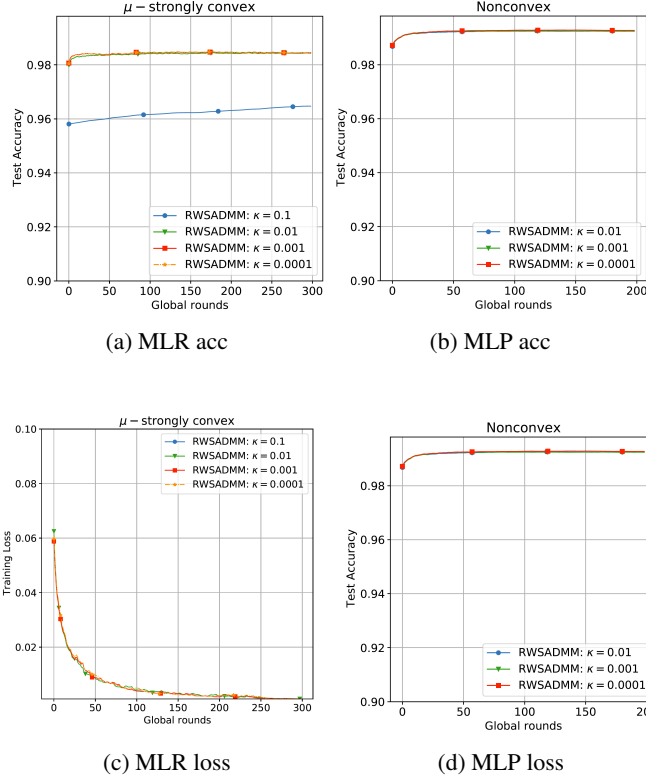


Figure 4: Effect of κ on the convergence of RWSADMM in the MLR (4a, 4c) and MLP (4b, 4d) models for MNIST dataset.

D.6 Different Number of Users

This appendix examines the effect of modifying the number of users/clients in the graph. The configuration values are all the same as the optional configuration for the RWSADMM algorithm with 20 agents. We keep the size of the neighborhood and the overall graph configurations the same for all the experiments. The batch size is decreased to 5 due to memory limitations, and the number of iterations is increased to 500. The total of users tested is 20, 50, and 100 users. The test accuracy and train loss progress curves for different numbers of clients are shown in Fig. 7.

As the number of users increases and the graph expands, the convergence gets more challenging, the test accuracy rates slightly decrease, and the time duration of the algorithm increases. The final test accuracy rates and time consumption of different graphs are presented in Table 2.

RWSADMM	MNIST	
	CNN	
# of users	acc(%)	t(s)
20	99.57	2929
50	99.25	6994
100	99.19	13878

Table 2: Test accuracy rate and time duration comparison of RWSADMM for different graphs with 20, 50, and 100 users/nodes in the graph.

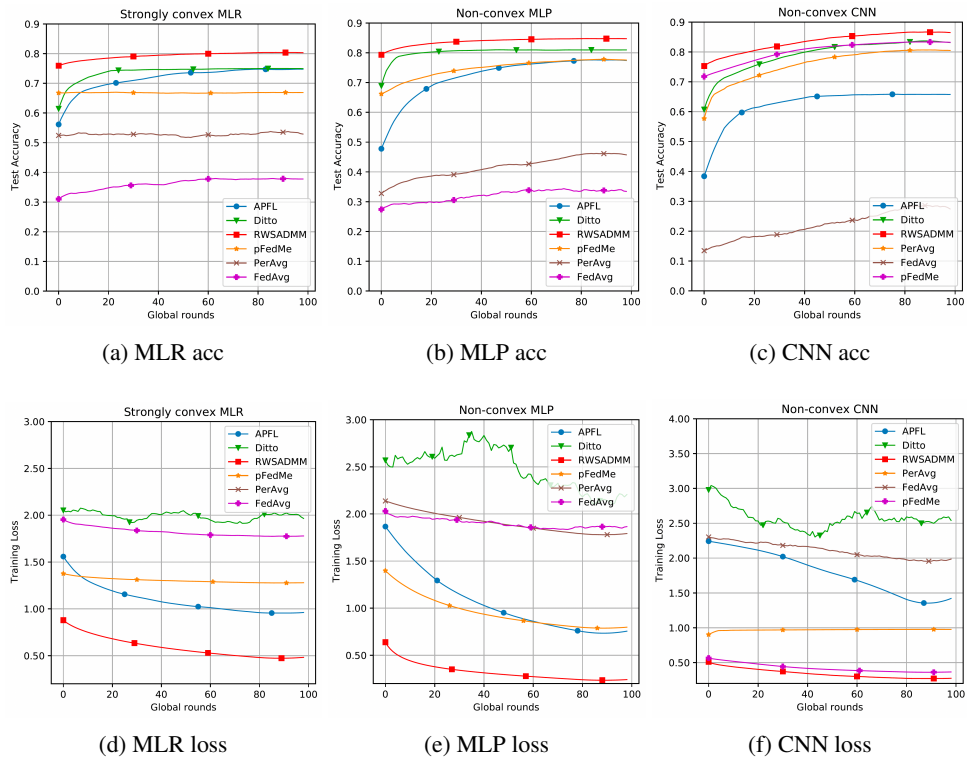


Figure 5: Performance comparison (test accuracy and training loss) of RWSADMM, pFedMe, PerAvg, FedAvg, APFL, and Ditto for CIFAR10 dataset for strongly convex MLR, non-convex MLP, and non-convex CNN models.

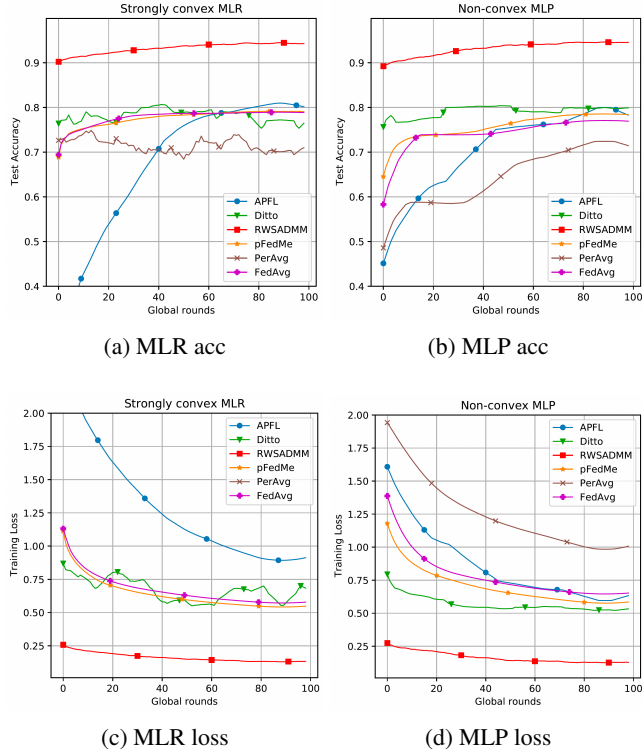


Figure 6: Performance comparison (test accuracy and training loss) of RWSADMM, pFedMe, PerAvg, FedAvg, APFL, and Ditto for Synthetic dataset and different settings: strongly convex MLR and non-convex MLP.

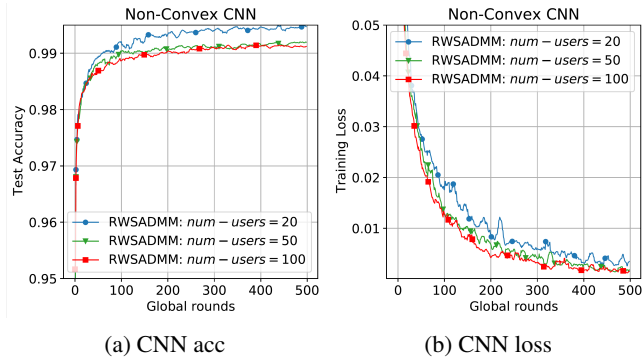


Figure 7: Performance comparison (test accuracy and training loss) of RWSADMM for different graphs with 20, 50, and 100 users/nodes in the graph.